9
Musculoskeletal

Standard Imaging Methods for Musculoskeletal Resions

A Spinal imaging methods

Overview

Conventional radiography is the first modality of choice if a lesion of the spine or spinal cord is suspected. MRI or CT is then performed to identify the lesion and determine its cause. MRI provides more information than CT and is therefore normally given priority. CT is performed if a detailed bone evaluation is required, and myelography and discography are also performed as necessary.

Detailed discussion

1. Conventional radiography

The standard imaging method includes imaging with 2 different projections, the anteroposterior and lateral projections. Both oblique views are added if foraminal stenosis or spondylolysis is suspected, for imaging with a total of 4 views. To evaluate spinal instability, as in the case of atlantoaxial subluxation and spondylolisthesis, imaging with the lateral views of anteflexion and retroflexion is added. Imaging with the open-mouth odontoid anteroposterior projection is added to evaluate odontoid fracture caused by cervical trauma, atlantoaxial destruction resulting from rheumatoid arthritis, and atlantoaxial rotatory fixation, which occurs preferentially in children.

2. Myelography and discography

Myelography is performed to evaluate spinal canal stenosis and spinal cord/nerve root sheath compression of various causes. Discography is performed for the morphological evaluation of intervertebral disks and for functional diagnosis by inducing or reproducing intervertebral disc pain. They are also performed in combination with CT (CT myelography, CT discography). The use of myelography and discography is becoming limited as MRI becomes more widely used.

3. CT

CT is performed to visualize fracture lines and calcification and ossification changes, such as ossification of the posterior longitudinal ligament, and intervertebral and intravertebral gas. It is also performed to evaluate spinal canal stenosis. The acquired slice thickness should be the thinnest possible for the system (≤ 1 mm). The 3 standard planes in which MPR images are generated are the transverse, sagittal, and coronal planes. Other planes are added as necessary. Three-dimensional imaging using the surface rendering shaded surface display (SSD) and the VR method is useful for showing complex structures in 3D. It is used when there is a need to understand 3D spatial relationships, such as in the case of atlantoaxial subluxation or

odontoid fracture. Because CT has a complementary relationship to MRI, their mutual strengths and weaknesses should be determined and used.

4. MRI

① Body position during imaging and coil used

Imaging is performed with the patient in the supine position. If the patient has scoliosis, the body axis is kept as straight as possible. When imaging of the cervical spine is performed, to avoid artifacts resulting from swallowing or cerebrospinal fluid and blood vessel pulsation, dentures are removed to minimize swallowing and neck movement. Although a phased array coil for the spine is used, use of a dedicated coil is not necessary with systems equipped with an in-table coil.

② Imaging sequences and planes

There are 2 standard imaging planes, the sagittal and transverse planes. For sagittal imaging, an imaging range that adequately includes the bilateral intervertebral foramina is set. T2-weighted sagittal imaging makes it easy to obtain an overview of the anatomy and lesions, and this is the imaging performed initially. T1-weighted sagittal imaging is useful for visualizing bone marrow lesions, lesions that show hyperintensity on T1-weighted images (e.g., hematomas, lipomas), and perineural cysts and for evaluating fat in the vertebral canal. With transverse imaging, the imaging cross-section selected varies according to the clinical signs and disease. In degenerative spinal disease, it is recommended that imaging at the intervertebral level and 3 slices above and below be selected. If a spinal cord or spinal canal lesion is suspected, the appropriate lesion levels are selected. If they are extensive, 1 cross-section each at the vertebral body and intervertebral levels should be selected. T2-weighted transverse imaging and $T2^*$-weighted transverse imaging are useful for evaluating spinal canal stenosis and the interior of the spinal canal. Compared with $T2^*$-weighted imaging, T2-weighted imaging has higher bone marrow lesion detection sensitivity and is less susceptible to magnetic susceptibility artifacts. However, a disadvantage of T2-weighted imaging is its susceptibility to artifacts caused by cerebrospinal fluid and blood vessel pulsation. Consequently, for imaging of the cervical and thoracic spine in degenerative spinal disease, $T2^*$-weighted imaging is recommended instead of T2-weighted imaging. If evaluation of the signal intensity of the lesion itself or of a spinal cord lesion is necessary, or the patient has metal implants, T2-weighted imaging is preferable. It should be noted, however, that $T2^*$-weighted imaging may overestimate spinal canal stenosis. T2-weighted imaging is recommended for transverse imaging of the lumbar spine. T1-weighted transverse imaging is useful when it is difficult to differentiate intervertebral disc herniation from the surrounding structures with T2- and $T2^*$-weighted imaging. It is also useful for seeing the relationship between a severely displaced intervertebral disc and the nerve root. Coronal imaging is useful for evaluating paraspinal lesions and the physical relationship between the nerve root, a protruding intervertebral disk, vertebral osteophytes, and a tumor. Fat-suppressed T2-weighted imaging and short-TI inversion recovery (STIR) imaging are excellent for detecting bone marrow lesions and perispinal lesions.

However, STIR imaging is even less susceptible to artifacts caused by metal than T2-weighted imaging, and it can provide stable fat suppression in areas where the magnetic field is non-uniform, such as the cervical and thoracic spine. For MR myelography, 2D and 3D methods are available. However, the 3D method, which provides good temporal resolution and contrast, is more widely used. MR myelography is used as an equivalent test to regular myelography, which is highly invasive. It enables good images of the lumbar spine to be obtained. However, in the cervical and thoracic spine, the subarachnoid space is narrow, and the images are susceptible to degradation caused by artifacts of cerebrospinal fluid pulsation and of magnetic field non-uniformity.

Table 1. Recommended parameters for MRI

Field of view (FOV)	Cervical and thoracic spine: 20 to 34 cm
	Lumbar spine: 16 to 20 cm
Slice thickness	Cervical spine: 3 to 4 mm
	Thoracic and lumbar spine: 4 to 5 mm
Matrix	256 to 512 ×132 to 270

Although the imaging parameters vary depending on the MR system, the important recommended parameters are shown in Table 1.

③ Standard imaging methods

The standard imaging methods must provide the ability to evaluate the bone marrow, intervertebral disks, spinal canal interior, and spinal cord. If a hematoma or tumorous lesion (e.g., tumor, cysts) is detected, the ability to perform qualitative diagnosis to some degree is necessary. The combination of sagittal and transverse imaging described above is recommended. The following are examples.

(1) Cervical spine (Fig. 1), thoracic spine

Sagittal imaging: T1-weighted imaging, T2-weighted imaging, and fat-suppressed T2-weighted or STIR imaging

Transverse imaging: T1-weighted imaging and $T2^*$-weighted or T2-weighted imaging

(2) Lumbar spine (Fig. 2)

Sagittal imaging: T1-weighted imaging, T2-weighted imaging, and fat-suppressed T2-weighted or STIR imaging

Transverse imaging: T1-weighted imaging, T2-weighted imaging

For cervical and thoracic spine transverse imaging, $T2^*$-weighted imaging is recommended in principle rather than T2-weighted imaging. However, if it is necessary to evaluate the signal intensity of the lesion itself or a spinal cord lesion, T2-weighted imaging should be performed. In investigating trauma, $T2^*$-weighted imaging is considered useful for detecting spinal cord injury (hemorrhage). Sagittal

T2*-weighted imaging should be added to the standard imaging method, and the transverse T2-weighted imaging should be changed to T2*-weighted imaging.

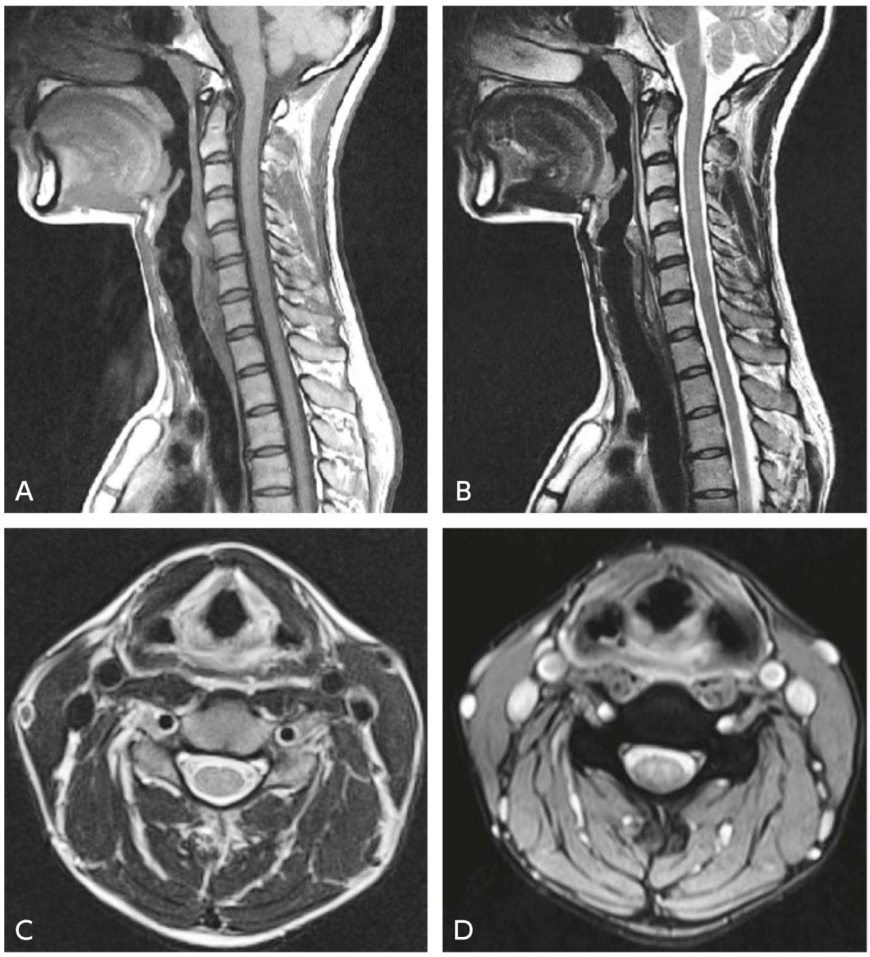

Figure 1. Cervical spine MRI

A: T1-weighted sagittal image, B: T2-weighted sagittal image, C: T2-weighted transverse image
D: T2*-weighted transverse image

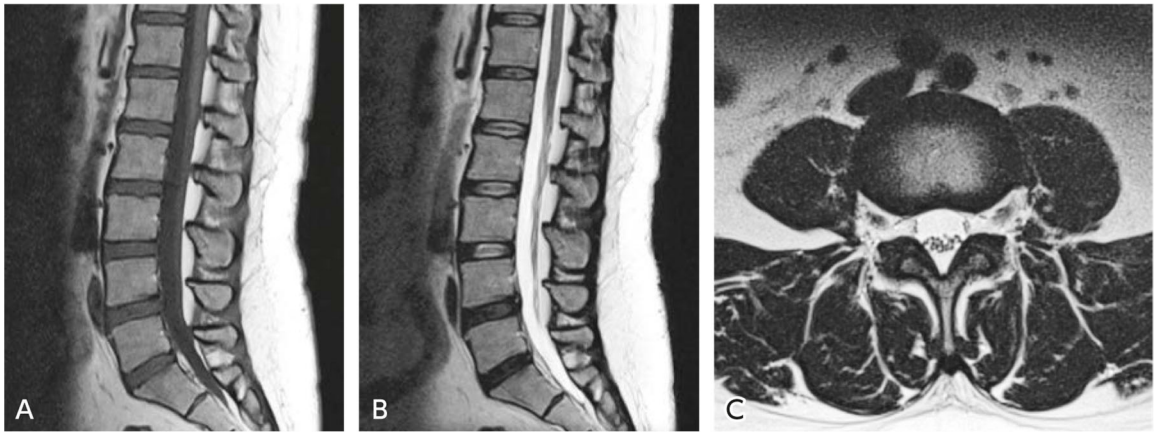

Figure 2. Lumbar spine MRI

A: T1-weighted sagittal image, B: T2-weighted sagittal image, C: T2-weighted transverse image

B Joint imaging methods

Overview

Conventional radiography remains the standard modality for diagnostic imaging of the joints. Although arthrography was previously performed for close investigation, its use has become limited with advances in imaging systems and their increased availability, and opportunities to use MRI in particular have increased. With MRI of the joints, it is considered necessary to evaluate small structures, and particular attention must be paid to the imaging range and cross-section selected and to the resolution. Unlike other areas, proton density-weighted imaging is commonly used for the joints. However, this imaging method is susceptible to image degradation resulting from blurring artifacts. To reduce this, a relatively short echo train length should be selected. The imaging methods for the various joints are described below.

Shoulder joint imaging methods

1. Conventional radiography

The standard imaging method involves imaging with 2 views, the anteroposterior and transverse views. Anteroposterior projection imaging is normally performed in the neutral position. Imaging with internal and external rotation is added as necessary. The lateral view of the scapula (Y view) is suitable for observing the inferior surface of the acromion. Imaging with this view is performed when diagnosing a rotator cuff tear or subacromial impingement. The internally rotated anteroposterior projection and flexion/semiaxial view (Stryker notch view) are useful for visualizing depressed fractures (Hill-Sachs lesions) of the posterolateral area of the humeral head, which occur with recurrent shoulder dislocation or subluxation. Imaging with the arm elevated (zero position) and with the upper arm hanging downward and under downward stress is useful for diagnosing joint laxity and loose shoulder. Imaging of the bicipital groove is performed to evaluate osteophyte protuberance and narrowing of the bicipital groove when long head of the biceps tendon injury and inflammation are suspected.

2. Arthrography

With the emergence of MRI, the use of contrast-enhanced imaging of the joint capsule and bursa to diagnose lesions of the soft tissue such as the rotator cuff and glenoid labrum has become limited. However, arthrography has advantages, such as permitting dynamic observations for investigating the cause of pain on movement, which is difficult with normal MRI, and it can be performed together with treatment for conditions such as joint distension (reduction of intra-articular pressure). Arthrography may also be performed in combination with CT and MRI (CT arthrography, MR arthrography).

3. CT

CT is performed for purposes such as evaluating bone fractures and visualizing joint mice and calcification. The acquired slice thickness should be the thinnest possible for the system (≤ 1 mm). The 3 standard planes in which MPR images are generated are the transverse, oblique sagittal parallel to the glenoid fossa, and oblique coronal perpendicular to the oblique sagittal. Other planes are added as necessary. For bone fractures, CT plays an ancillary role to conventional radiography and can be used to evaluate aspects such as the presence or absence of fracture lines, the number and location of bone fragments, the direction of displacement, and the condition of the joint surface. Three-dimensional images generated using the SSD and VR methods are suitable for determining the nature of bone fractures and dislocations. They are useful for purposes such as the preoperative planning of fracture reduction, osteosynthesis, and functional reconstructive surgery. CT arthrography may be performed to evaluate intra-articular structures such as the glenoid labrum and joint-side rotator cuff.

4. MRI

① Body position during imaging and coil used

The body position during imaging is supine, with the arms in an unstrained, natural, neutral to mildly externally rotated position and the palms of the hands facing the trunk. However, it should be noted that external rotation of the arms may cause pain. Material such as sponge is used to reduce artifacts caused by movement, and the shoulder joint is held in place with a shoulder coil (e.g., phased-array coil or flex coil). A device such as a bust band is used to address respiratory movement. Because the shoulder joint is located laterally on the body and away from the center of the gantry, some means of positioning and increasing the static magnetic field uniformity needs to be devised.

② Imaging sequences and plan

Although T2-weighted imaging is useful for evaluating the rotator cuff, its sensitivity in detecting glenoid labrum lesions is low. $T2^*$-weighted imaging is useful for evaluating the glenoid labrum. However, because false lesions can appear even in a normal glenoid labrum due to the magic angle effect, caution is required in such evaluations. Moreover, bone marrow lesions are indistinct with these imaging methods. Fat-suppressed, $T2^*$-weighted imaging and STIR imaging enable lesions to be visualized in soft tissue, including the rotator cuff, and bone marrow with high sensitivity. Proton density-weighted imaging is useful for evaluating the rotator cuff and glenoid labrum. However, false lesions can also appear in the rotator cuff with this modality due to the magic angle effect, and caution is therefore required in such evaluations. Although T1-weighted imaging provides little information, it is useful for evaluating the bone marrow and incidental abnormal findings, such as hematomas and tumorous lesions (e.g., tumors and cysts).

Table 2. Recommended parameters for MRI

Field of view (FOV)	15 to 18 cm
Slice thickness	3 to 4 mm
Matrix	256 × 230
Echo train length for proton density-weighted imaging	4 to 6

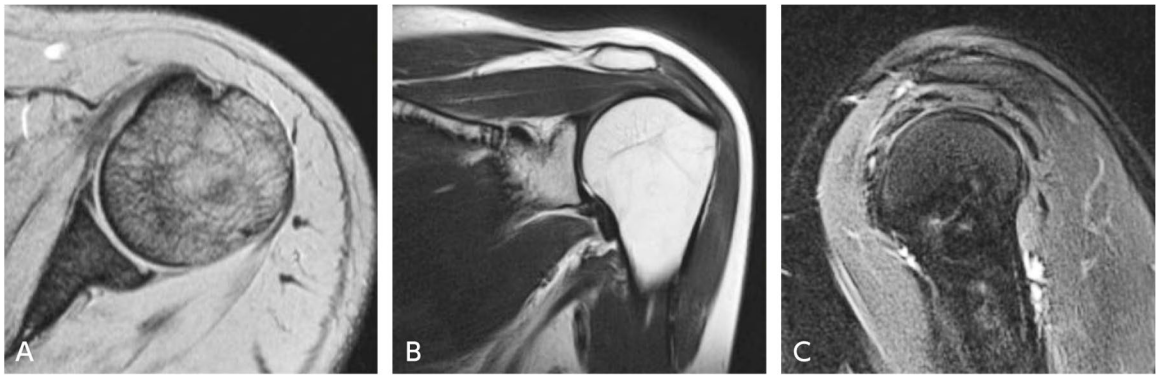

Figure 3. Shoulder joint MRI

A: T2*-weighted transverse image, B: T2-weighted oblique coronal image, C: Fat-suppressed, T2-weighted oblique sagittal image

There are 3 standard imaging planes, the transverse, oblique coronal, and oblique sagittal planes. Transverse imaging is performed perpendicular to the glenoid fossa (or trunk axis) and humerus (or trunk axis) and includes the area from the acromioclavicular ligament to the subscapularis muscle. Oblique coronal imaging is performed parallel to the supraspinatus muscle and includes the area from the infraspinatus muscle to the subscapularis muscle. For oblique sagittal imaging, imaging perpendicular to the glenoid fossa is specified and includes the area from the deltoid muscle to the center of the scapula. In abduction and external rotation, oblique transverse imaging is performed from the coronal scout parallel to the long-axis of the humerus. Oblique coronal and oblique sagittal imaging are added as appropriate. The imaging views useful for the shoulder's essential components/structures are as follows: oblique coronal and oblique sagittal imaging for the rotator cuff, oblique sagittal and oblique coronal imaging for the intra-articular long head of the biceps tendon, transverse imaging for the bicipital groove, oblique sagittal and transverse imaging for the glenohumeral ligaments and rotator cuff interval, and transverse and oblique coronal imaging for the glenoid labrum. The 3 standard imaging views are added complementarily for diagnosis.

Although the imaging parameters vary depending on the MR system, the important recommended parameters are shown in Table 2.

③ Standard imaging method

The standard imaging methods must permit evaluation of the bone marrow and the stabilizing mechanism, including the rotator cuff, the long head of the biceps tendon, and the glenoid labrum. T2-weighted imaging and T2*-weighted imaging are considered fundamental, and fat-suppressed,

T2-weighted imaging from at least 1 plane is desirable. T1-weighted imaging is considered for bone marrow evaluation and when a hematoma or tumorous lesion is present and should be performed from 1 plane. The imaging methods to be used are determined based on the above considerations. Examples are shown below (Fig. 3).

Oblique coronal imaging: T1-weighted imaging, T2-weighted imaging, or fat-suppressed, T2-weighted imaging*

Oblique sagittal imaging: T2-weighted imaging or fat-suppressed, T2-weighted imaging*

(*Combination of oblique coronal, T2-weighted imaging and oblique sagittal, fat-suppressed, T2-weighted imaging or oblique coronal, fat-suppressed, T2-weighted imaging and oblique sagittal, T2-weighted imaging)

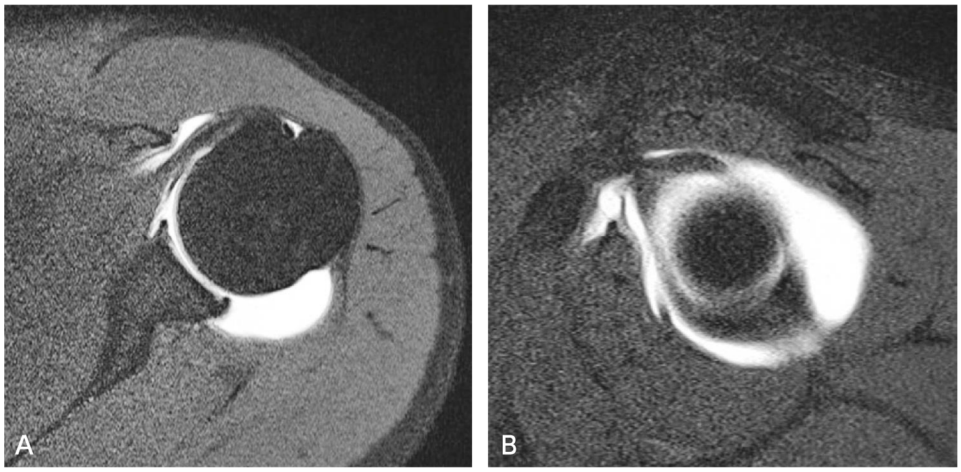

Figure 4. Shoulder joint (direct MR arthrography)

A: Fat-suppressed T1-weighted transverse image, B: Fat-suppressed T1-weighted oblique sagittal image

④ MR arthrography

MR arthrography is used to evaluate injury to intra-articular structures such as the glenoid labrum, long head of the biceps tendon/labrum complex, glenohumeral ligaments, and joint-side rotator cuff. MR arthrography encompasses direct MR arthrography, wherein imaging is performed after a diluted solution of contrast medium is injected into the joint, and indirect MR arthrography, wherein imaging is performed with an exercise load applied after intravenous administration. In direct MR arthrography, imaging is performed after 10 to 20 mL of gadolinium contrast medium diluted 100-fold to 250-fold with physiological saline are injected into the joint (Fig. 4). Although it is invasive, it provides adequate expansion of the joint capsule. Indirect MR arthrography, although minimally invasive, has disadvantages, such as the need for an exercise load, inadequate expansion of the joint capsule, and hindrance of the evaluation by soft tissue contrast enhancement. Direct MR arthrography is more commonly performed.

Fat-suppressed, T1-weighted imaging is performed from the 3 standard angles, with imaging in external rotation and abduction added as appropriate. However, this position may induce pain and cannot be used for all patients. Injury to intra-articular structures can be evaluated based on contrast medium leakage and infiltration. To differentiate between intra- and extra-articular fluid accumulations, additional fat-suppressed, T2-weighted imaging should be performed for any plane.

⑤ Intra-articular contrast medium administration

Currently, only 1 iodine contrast medium is approved for intra-articular administration in Japan. The package inserts for gadolinium contrast media do not mention intra-articular administration. The intra-articular administration of gadolinium contrast media is widely accepted not only in Japan, but throughout the world. However, when performing MR arthrography, such use must be clearly explained to the patient in advance and the patient's consent obtained.

Elbow joint imaging methods

1. Conventional radiography

The standard imaging method includes imaging with 2 different projections, the anteroposterior and lateral projections. Anteroposterior projection imaging should be obtained with the elbow extended. Lateral view imaging is performed with elbow flexion at 90 degrees. In both views, the forearm is in a neutral position with respect to rotation. Oblique projection is useful for detecting bone fractures that are hard to discern, particularly fractures of the radial head, the coronoid process of the ulna, and the lateral epicondyle in children. For osteochondritis dissecans of the humeral capitulum, anteroposterior projection with flexion of 45 degrees provides better visualization of lesions than normal anteroposterior projection. Osteophyte formation and ulnar groove deformation in cubital tunnel syndrome are observed by ulnar groove projection. Valgus/varus stress radiography is performed to evaluate instability resulting from injury of the medial and lateral collateral ligaments. Comparison by imaging of the unaffected side is useful in the case of trauma in a child when assessment is uncertain. However, caution is required with respect to increased radiation exposure.

2. Arthrography

Because MRI has improved demonstration of the structural components of the joint, the use of arthrography is limited. In the case of a partial rupture of the medial collateral ligament, penetration of contrast medium into the ruptured area is seen on CT or MR arthrography, and detection of ligament injury is better than with noncontrast tests.

3. CT

CT is often performed to determine the presence or absence of a fracture in acute trauma, the condition of the joint surface, displaced bone fragments, and to conduct a detailed investigation of loose bodies or

osteophytes that could restrict the range of motion of the joint. MPR images of the joint surface are generated in 3 planes, transverse, sagittal, and coronal. However, to permit high-resolution image reconstruction from all angles, the slice thickness selected is the minimum for the system used (≤ 1 mm). In this case, a reconstruction slice thickness of 2 mm is selected. VR imaging is useful for purposes such as preoperative simulation. However, depending on the setting of the threshold it can be difficult to visualize small fractures and loose bodies. Consequently, it is used to complement MPR.

4. MRI

① Body position during imaging and coil used

Imaging is performed in the supine position with the elbow extended and the arm lowered. For good visualization of the collateral ligaments, forearm rotation in relation to the upper arm is minimized. If the patient is physically large, the elbow joint may be at the edge of the gantry and outside the center of the static magnetic field, resulting in poor image quality. In this case, the patient is tilted so that the elbow joint moves closer to the center. Although there is a method that involves having the patient raise the imaged arm while in the prone position, this places a burden on the shoulder joint, making the imaging susceptible to artifacts caused by movement. It is important to confirm that the subject is in a position that allows him or her to remain still, and that the test can be performed comfortably.

A round or rectangular coil and a coil for the hand and elbow are used. When examining intra-articular structures in detail, a small round coil or coil for the hand and elbow that is 7 to 8 cm in diameter is used to increase spatial resolution.

② Imaging sequences and planes

The imaging sequences vary depending on the target structure. If the target is a ligament, $T2^*$-weighted imaging, fat-suppressed, T2-weighted imaging or STIR imaging, and proton density-weighted imaging are suitable. For detailed examination of the common tendons of the extensor and flexor muscles, T2-weighted imaging and fat-suppressed, T2-weighted imaging or STIR imaging are useful. For detection of bone injury, STIR imaging and fat-suppressed, T2-weighted imaging are highly sensitive, and T1-weighted imaging is excellent for evaluating fracture lines and intra-articular hematomas. For evaluating articular cartilage, fat-suppressed, proton density-weighted imaging, 3D, fat-suppressed, GRE-T1-weighted imaging, and 3D GRE with water-selective sequence are useful. When imaging the elbow joint, the area being imaged is at the edge of the magnetic field. Consequently, STIR imaging often provides better fat suppression than fat-suppressed, T2-weighted imaging.

There are 3 standard imaging planes, the transverse, coronal, and sagittal planes. For transverse imaging, the area from the distal metaphysis of the humerus to the radial tuberosity is imaged. Coronal imaging is set to be performed parallel to a straight line from the medial epicondyle to the lateral epicondyle or a straight line across the anterior border, as seen in a transverse image acquired at the level of the distal metaphysis of the humerus (Fig. 5). The sagittal plane is the plane perpendicular to the coronal plane.

Although the imaging parameters vary depending on the MR system, the recommended parameters are shown in Table 3. During 3D data acquisition by GRE, a slice thickness of ≤2 mm can be selected, allowing images of higher spatial resolution to be obtained.

③ Standard imaging methods

It is important that the standard imaging methods enable the lateral collateral ligament, tendon origins, and bone marrow to be evaluated. Coronal imaging is useful for evaluating the lateral collateral ligament and tendon origins. Transverse imaging is performed to evaluate soft tissue, particularly muscle. STIR and fat-suppressed, T2-weighted imaging are useful for evaluating various structures. At a minimum, coronal and transverse imaging should be performed. T1-weighted imaging is useful for evaluating bone marrow, hematomas, and tumorous lesions. Coronal or sagittal T1-weighted imaging is recommended. The imaging duration is approximately 30 minutes. The imaging methods to be used are determined based on the above considerations. Examples are shown below.

Coronal imaging: $T2^*$-weighted imaging, fat-suppressed, T2-weighted or STIR imaging, and proton density-weighted imaging

Sagittal imaging: T1-weighted imaging and fat-suppressed, T2-weighted or STIR imaging

Transverse imaging: STIR imaging

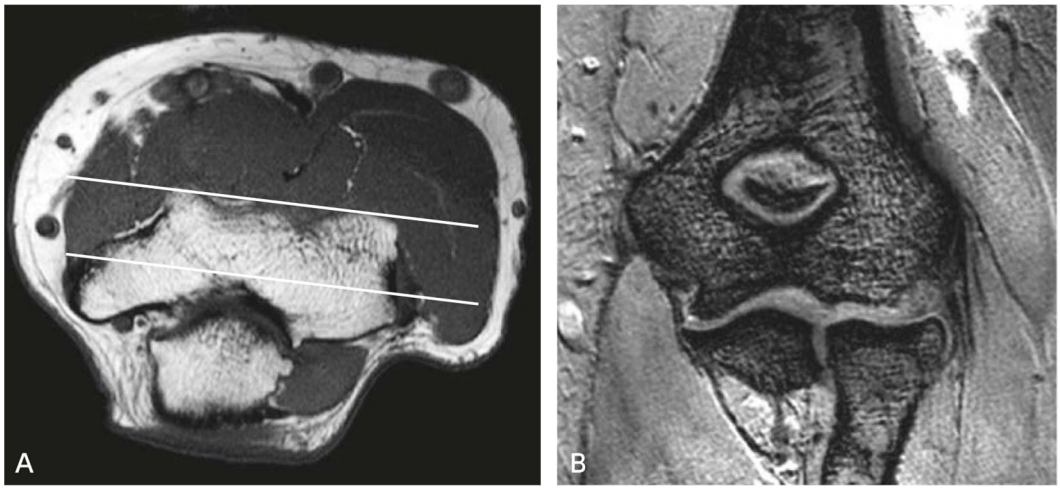

Figure 5. Elbow joint MRI

A: T1-weighted transverse imaging, B: $T2^*$-weighted coronal imaging

Table 3 Recommended parameters for MRI

Field of view (FOV)	10 to 14 cm
Slice thickness	3 to 4 mm
Matrix	256 × 230〜204
Echo train length for proton density-weighted imaging	4 to 6

If detailed demonstration of the articular cartilage is required, sagittal, fat-suppressed, proton density-weighted imaging, 3D, fat-suppressed, GRE-T1-weighted imaging, or 3D GRE with water-selective sequence imaging can be added. $T2^*$-weighted imaging is useful for detecting small loose bodies in patients with restricted range of motion, as in the case of a throwing injury or locking.

Hand and wrist joint imaging methods

1. Conventional radiography

The standard imaging views for conventional radiography of the hand and wrist joint are the anteroposterior and lateral views, with other imaging methods added as necessary. For example, scaphoid fractures frequently occur in the waist of the scaphoid bone, and the anteroposterior projection of ulnar flexion, which enables the scaphoid bone to be evaluated along its long axis, is useful in this case. In addition, the oblique view with pronation of 45 degrees to 60 degrees clearly shows fractures between the center of the bone and its distal end. Fractures of the uncinate process of the hamate bone are diagnosed by carpal tunnel imaging. In evaluating carpal instability, accurate lateral view imaging in the neutral position is necessary to measure the scapholunate angle (normally 30 degrees to 60 degrees).

2. Arthrography

Arthrography is used to evaluate the triangular fibrocartilage and the scapholunate and lunotriquetral ligaments. Imaging of 3 compartments, the radiocarpal joint, distal radioulnar joint, and middle carpal joint, is considered the standard imaging method. However, imaging of the radiocarpal joint alone has been shown to provide equal diagnostic performance. Problems with arthrography are that it is of limited usefulness for evaluating radial carpal pain, accurately identifying sites of ligament damage with it is difficult, and it provides no information on the severity of damage. In addition, false positives (degenerative changes can produce a positive test) and false negatives (ligament injury without intercompartmental communication cannot be diagnosed) are problematic.

3. CT

CT is performed to diagnose microscopic and complicated bone fractures and to perform detailed evaluations, such as the evaluation of bone fracture healing. A slice thickness of approximately 1 mm is desirable. Multiplanar reconstruction imaging is very useful for these evaluations. It enables images to be generated not only in the transverse, sagittal, and coronal planes, but in planes that suit the purpose of the testing. Three-dimensional reconstruction imaging (SSD or VR) is used to elucidate the locations of lesion sites in three dimensions.

4. MRI

MRI permits detailed evaluation of the structure of the complex bone and soft tissue of the carpal region and fingers. The recent development of high magnetic fields and coil technology has made it possible to

visualize structures such as ligaments, tendons, and nerves clearer than before and contributed to improved diagnostic accuracy.

① Body position during imaging and coil used

If one hand is being imaged, imaging is performed with the patient prone and the hand raised above the head and fixed in place (“superman” position). If this position is difficult for the patient to maintain, imaging is performed with the patient supine, the elbow extended, and the hand fixed in place alongside the body. To image the hand as close as possible to the center of the MRI table, a lateral position may be used. Although the use of a small round coil is standard, a suitable coil is selected for imaging of the entire hand or both hands.

② Imaging sequences and planes

The main imaging sequences used are T1-, T2-, and $T2^*$-weighted imaging and proton density-weighted imaging. Fat suppression is concurrently used as appropriate. Because STIR imaging provides uniform fat suppression, the 3D-GRE method, which is frequently used for the same purpose as fat-suppressed, T2-weighted imaging, is advantageous for visualizing fine structures and evaluating the blooming that occurs in relation to hemorrhage. Post-contrast, fat-suppressed, T1-weighted imaging may provide useful information for evaluating tumors, tumor-like conditions, and infectious diseases such as rheumatoid arthritis and infection. When the imaged site is definable, imaging is performed with a coil such as a small round coil and the FOV narrowed to approximately 6 cm. The slice thickness used is approximately 2 to 3 mm for 2D imaging and approximately 1 mm for 3D imaging, with a matrix size of $\geq 256 \times 256$. Diffusion-weighted imaging is not generally used.

Evaluation by transverse imaging is the standard evaluation for rupture of an extensor or flexor tendon. Sagittal imaging is useful for evaluating long-axis views. In the case of collateral ligament injury, the imaging plane must be correctly set to the coronal plane suitable for the joint, and particular caution is required to determine the position in the case of thumb collateral ligament injury (Fig. 6). For intercarpal ligament or triangular fibrocartilage complex (TFCC) injury, coronal plane imaging is standard, with sagittal imaging used complementarily. Two-dimensional or 3D-GRE sequences are added. Carpal fracture is evaluated by transverse, coronal, and sagittal imaging. Transverse imaging is useful for hamate fractures.

Figure 6. Thumb MRI

A: T1-weighted transverse imaging, B: Fat-suppressed, T2-weighted coronal imaging
Correctly specifying coronal imaging for the metacarpophalangeal (MP) joint facilitates collateral ligament injury (→) diagnosis.

For detailed examination of rheumatoid arthritis, both hands should be imaged simultaneously when possible. However, there is no consensus on the appropriate limb position for imaging. If there are equipment (coil) limitations, only 1 hand is included in the imaging range. In any event, firm immobilization of the hand and the subject's cooperation are essential to minimize body movement artifacts. T1-weighted imaging is useful for evaluating destructive changes, fat-suppressed, T2-weighted imaging and STIR imaging are useful for evaluating bone marrow edema, and post-contrast, fat-suppressed, T1-weighted imaging is useful for evaluating synovitis. Dynamic contrast-enhanced MRI, while not essential, is useful for characterization, including determining the status of a condition. The selection of the imaging sequence is also an important factor in obtaining good image quality. Imaging in the coronal plane is standard, with transverse plane imaging added as appropriate.

Hip joint imaging methods

1. Conventional radiography

The standard imaging method involves imaging from 2 views, the anteroposterior projection and the lateral view of the femur of the hip being examined. The anteroposterior projection imaging is performed with the hip extended and the leg slightly internally rotated. With the leg internally rotated, the femoral neck faces frontward, making superimposition of the greater and lesser trochanters unlikely. The lateral view of the femur is useful for evaluating femoral neck fractures, femoral head osteonecrosis, Perthes' disease, and slipped femoral capital epiphysis. In adults, anteroposterior projection imaging is performed with flexion of 90 degrees and abduction of 45 degrees. Oblique view imaging is performed with the pelvis inclined 45 degrees toward the hip being examined, flexion of 90 degrees, and abduction of 45 degrees

(Lauenstein view or a modified version of it). Axial view imaging is performed with the asymptomatic hip in flexion and the hip being examined in extension. Transverse view imaging can also be performed if a factor such as pain makes flexion and abduction of the hip being examined difficult. In children, imaging in the frog-leg view is common. Anteroposterior projection imaging with adduction or abduction is used as dynamic imaging to evaluate the fit of the acetabulum and femoral head.

2. Arthrography

Arthrography is performed mainly to evaluate the articular cartilage, acetabular lip, and joint mice. Concomitant CT or MRI (CT and MR arthrography) is useful for their detailed evaluation. However, because arthrography is invasive, its indications are limited.

3. CT

CT is performed for purposes such as evaluating bone fractures (evaluation of fracture morphology, bone fragment displacement, and condition of articular surface; visualization of small bone fragments) and visualizing joint mice and calcification. The acquired slice thickness should be the thinnest possible for the system (≤ 1 mm). The 3 standard planes in which MPR images are generated are the transverse, sagittal, and coronal planes. Other planes are added as necessary. Three-dimensional images generated using the SSD and VR methods are useful for determining the nature of bone fractures and dislocations in 3D. In osteoarthritis and femoral head osteonecrosis, CT may be used for a preoperative simulation of joint replacement surgery, as well as for evaluating bone morphology.

4. MRI

① Body position during imaging and coil used

MRI is normally performed in the supine position using a body coil and includes the bilateral hip joints. Use of a phased-array coil enables images with a high SNR to be obtained. A local coil is used if detailed evaluation of structures such as the acetabular lip and articular cartilage is required for only 1 hip joint.

② Imaging sequences and planes

T1-weighted imaging is useful for evaluating the bone marrow and incidental abnormal findings, such as hematomas and tumorous lesions (e.g., tumors and cysts). Proton density-weighted imaging and $T2^*$-weighted imaging are suitable for evaluating the acetabular lip. However, bone marrow lesions are indistinct with these modalities. T2-weighted imaging has low visualization sensitivity for the acetabular lip, and bone marrow lesions are indistinct with this modality. However, it is useful for visualizing joint fluid accumulation and fracture lines. Fat-suppressed, T2-weighted imaging and STIR imaging enable lesions to be visualized in soft tissue and bone marrow with high sensitivity.

The following modalities are useful for evaluating articular cartilage: proton density-weighted imaging, fat-suppressed, proton density-weighted imaging, T2-weighted imaging, and 3D, fat-suppressed,

GRE-T1-weighted imaging or 3D selective water excitation GRE-T1 weighted imaging. Three-dimensional, fat-suppressed, GRE-T1-weighted imaging, and 3D selective water excitation, GRE-T1-weighted imaging enable thin MPR images to be generated in any arbitrary plane, making these modalities suitable for detailed evaluation of the morphology and thickness of the articular cartilage.

Table 4. Recommended parameters for MRI

Field of view (FOV)	Bilateral: 32 to 40 cm Unilateral: 14 to 18 cm
Slice thickness	3 to 4 mm
Matrix	256 × 230 to 256
Echo train length for proton density-weighted imaging	4 to 6

There are 3 standard imaging planes, the coronal, sagittal, and transverse planes. The most standard of these is the coronal plane. Coronal and transverse imaging enable left-right comparisons, and coronal imaging can be used to evaluate the pelvis as a whole. Sagittal imaging is suitable for evaluating the anterior and posterior of the epiphysis and acetabulum.

Although the imaging parameters vary depending on the MR system, the important recommended parameters are shown in Table 4.

③ Standard imaging methods

The standard imaging methods must provide the ability to evaluate the bone marrow, including that of the femoral head, the acetabular lip, and the articular cartilage. Fat-suppressed, proton density-weighted imaging is useful for evaluating various structures and should be performed in the coronal plane. T1-weighted imaging is considered for bone marrow evaluation and when a hematoma or tumorous lesion is present. It should be performed in the coronal plane. Fat-suppressed, T2-weighted imaging and STIR imaging enable lesions to be visualized in soft tissue and bone marrow with high sensitivity. Imaging from 1 or more angles is recommended with these modalities. T2-weighted imaging should also be performed from 1 or more angles.

The imaging sequences to be used are determined based on the above considerations. Examples (Fig. 7) are shown below.

Coronal imaging: T1-weighted imaging, T2-weighted imaging, fat-suppressed, proton density-weighted imaging

Sagittal imaging: T2-weighted imaging

Transverse imaging: Fat-suppressed, T2-weighted or STIR imaging

If femoral head osteonecrosis is suspected, or the imaging is performed to examine it in detail, sagittal T2-weighted imaging should be changed to T1-weighted imaging.

Knee joint imaging methods

1. Conventional radiography

The standard imaging method includes imaging with 2 different projections, the anteroposterior and lateral projections. Anteroposterior projection imaging is performed in extension with the leg slightly inwardly rotated. Lateral view imaging is performed with flexion of 30 degrees. Patellar axial view imaging (skyline view) is added to evaluate the patellofemoral joint. Axial dynamic imaging, in which the patellar axial view imaging is performed with flexion of 30, 60, and 90 degrees, is useful for evaluating the fit of the articular surface of the patellofemoral joint. Standing anteroposterior projection imaging enables the thickness of the articular cartilage of the femoral neck joint to be visualized as the width of the joint cleft, making it useful for evaluating the thickness of the cartilage. Imaging should be performed with the patient standing on the one leg that is being examined. If this is difficult, however, imaging is performed with the patient standing on both legs. Anteroposterior projection imaging in flexion (intercondylar fossa view) is useful for visualizing osteochondritis dissecans, joint mice, and avulsion fractures at cruciate ligament insertion sites. Valgus/varus stress radiography is performed to evaluate instability resulting from medial and lateral collateral ligament injuries. Anterior/posterior drawer radiography is performed to evaluate instability resulting from anterior cruciate ligament injury/posterior cruciate ligament injury.

2. Arthrography

Because arthrography is invasive and requires skill to perform, it is being replaced by MRI. Arthrography may also be performed in combination with CT and MRI (CT arthrography, MR arthrography) to evaluate the articular cartilage and visualize joint mice.

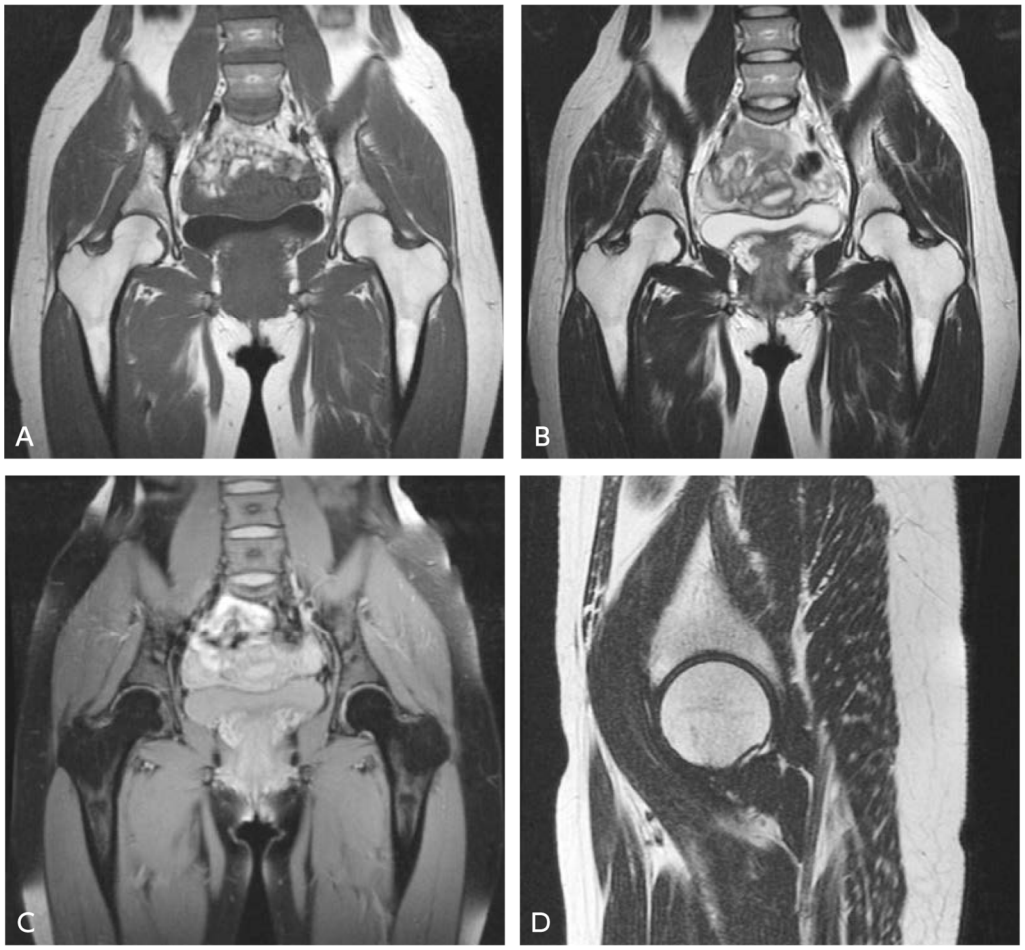

Figure 7. Hip joint MRI

A: T1-weighted coronal image, B: T2-weighted coronal image, C: Fat-suppressed, proton density-weighted, coronal image
D: T2-weighted sagittal image

3. CT

CT is performed for purposes such as evaluating bone fractures (evaluation of fracture morphology, bone fragment displacement, and condition of articular surface; visualization of small bone fragments), evaluating osteochondral injury, and visualizing joint mice and calcification. The acquired slice thickness should be the thinnest possible for the system (≤ 1 mm). The 3 standard planes in which MPR images are generated are the transverse, sagittal, and coronal planes. Other planes are added as necessary. Fracture lines are distinctly visualized in a plane perpendicular to the fracture line. Three-dimensional images generated using the SSD and VR methods are useful for determining the nature of bone fractures and dislocations in 3D.

4. MRI

① Body position during imaging and coil used

Imaging in slight flexion rather than full extension is recommended to distinctly visualize the anterior cruciate ligament. To avoid torsion on the cruciate ligaments and lateral collateral ligament, excessive

internal rotation and external rotation are avoided, and imaging is performed in a comfortable position with the leg in slight external rotation. A cylindrical knee coil is used.

② Imaging sequences and planes

Although T2-weighted imaging is useful for evaluating tendons and ligaments, its sensitivity in detecting meniscal injury is low. Proton density-weighted imaging is suitable for evaluating the menisci, tendons, and ligaments. However, false lesions can appear in normal tendons and ligaments that are at a 55-degree angle with respect to the static magnetic field due to the magic angle effect, and caution is therefore required in such evaluations. $T2^*$-weighted imaging is useful for evaluating the menisci. Its sensitivity in visualizing meniscal injury is higher than that of proton density-weighted imaging. Three-dimensional, $T2^*$-weighted imaging enables MPR images to be generated in thin planes and any arbitrary plane, making it excellent for visualizing small ruptures and evaluating rupture morphology. Bone marrow lesions are indistinct with T2-weighted, proton-weighted, and $T2^*$-weighted imaging. Fat-suppressed, T2-weighted imaging and STIR imaging enable lesions to be visualized in bone marrow and soft tissue, including tendons and ligaments, with high sensitivity. Although T1-weighted imaging provides little information, it is useful for evaluating the bone marrow and incidental abnormal findings, such as hematomas and tumorous lesions (e.g., tumors and cysts).

Table 5. Recommended parameters for MRI

Field of vision (FOV)	12 to 16 cm
Slice thickness	3 to 4 mm†
Matrix	256 × 230 to 256
Echo train length for proton density-weighted imaging	4 to 6

† ≤ 1 mm for 3D $T2^*$-weighted imaging

The imaging sequences useful for evaluating articular cartilage with general MR systems are proton density-weighted imaging, fat-suppressed, proton density-weighted imaging, T2-weighted imaging, 3D, fat-suppressed, GRE-T1-weighted imaging, and 3D selective water excitation, GRE-T1 weighted imaging. Three-dimensional, fat-suppressed, GRE-T1-weighted imaging, and 3D selective water excitation, GRE-T1-weighted imaging enable thin MPR images to be generated in any arbitrary plane, making these sequences suitable for detailed evaluation of the morphology and thickness of the articular cartilage. They are also used to evaluate the volume of the articular cartilage. In addition, sequences such as delayed gadolinium-enhanced magnetic resonance imaging of cartilage (dGEMRIC), T2 mapping, and T1 rho mapping have been proposed to evaluate qualitative changes in cartilage (collagen degeneration and decreased proteoglycans), the MR systems that can perform these imaging sequences are limited, and their clinical usefulness has not been established.

There are 3 standard imaging planes, the sagittal, coronal, and transverse planes. The menisci are evaluated in the sagittal and coronal planes, tendons and ligaments in the 3 standard planes, the articular cartilage of the femorotibial articulation in the sagittal and coronal planes, and the articular cartilage of the

patellofemoral joint in the sagittal and transverse planes. Although the imaging parameters vary depending on the MR system, the important recommended parameters are shown in Table 5.

③ Standard imaging methods

Most knee joint MRI is performed to closely examine internal derangement and trauma of the knee. The standard imaging methods must provide the ability to evaluate the menisci, ligaments, articular cartilage, and bone marrow. Sagittal T2-weighted imaging and proton density-weighted imaging elucidate the anatomy of the intra-articular structures, and one of them should therefore be performed. Fat-suppressed, proton density-weighted imaging is suitable for evaluating various structures, and its use in any plane is recommended. However, its sensitivity in detecting meniscal tears is slightly lower than that of $T2^*$-weighted imaging. It is recommended that at least $T2^*$-weighted imaging in either the sagittal or coronal plane and fat-suppressed, proton density-weighted imaging from 1 or more angles be performed. T1-weighted imaging is considered for bone marrow evaluation and when a hematoma or tumorous lesion is present. It should be performed from 1 angle. The imaging sequences to be used are determined based on the above considerations. Examples are shown below.

(1) Example 1 (Fig. 8)

Sagittal imaging: T2- and $T2^*$-weighted imaging†

Coronal imaging: T1-weighted and fat-suppressed, proton density-weighted imaging

Transverse imaging: Fat-suppressed, proton density-weighted imaging

(2) Example 2

Sagittal imaging: T1- and proton density-weighted imaging

Coronal imaging: $T2^*$-weighted imaging* and fat-suppressed, T2-weighted or STIR imaging

Transverse imaging: Fat-suppressed, proton density-weighted imaging

(† $T2^*$-weighted imaging performed in 3D and MPR image generation that includes the sagittal and coronal planes is preferable)

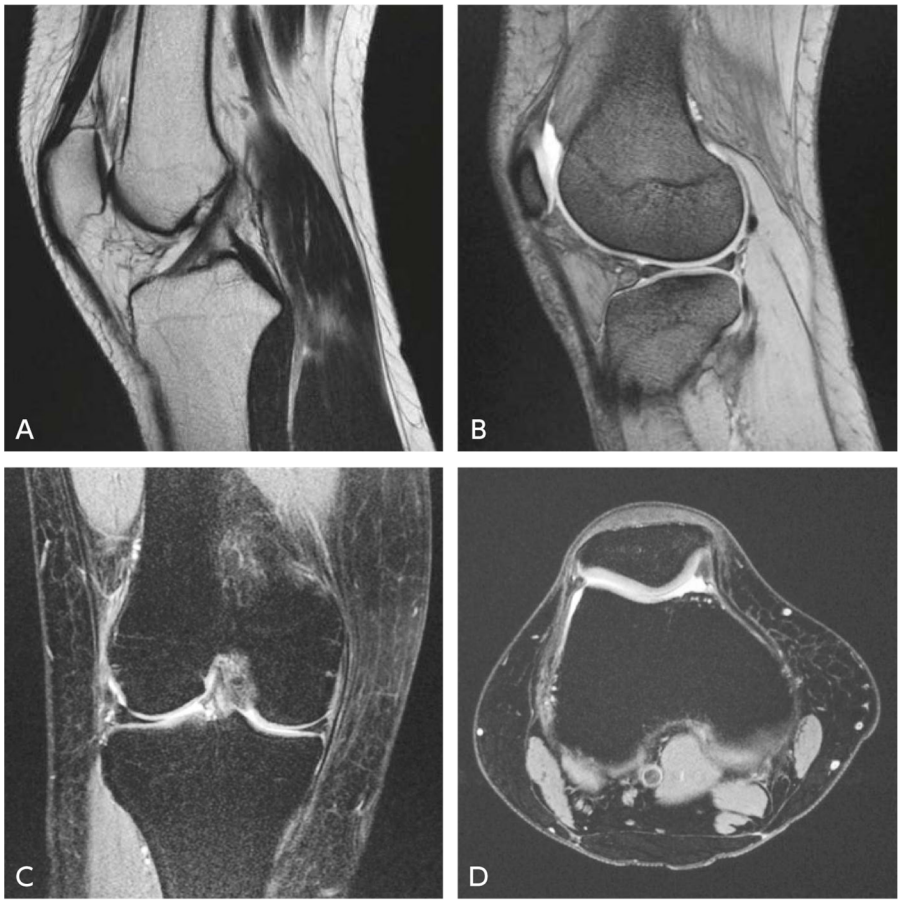

Figure 8. Knee joint MRI

A: T1-weighted sagittal image, B: T2*-weighted sagittal image, C: Fat-suppressed, proton density-weighted coronal image
D: Fat-suppressed, proton density-weighted transverse image

The addition of sagittal fat-suppressed, T2-weighted imaging or STIR imaging is recommended if anterior knee pain is present or extensor mechanism impairment is suspected. If a detailed evaluation of the articular cartilage is required, 3D, fat-suppressed, GRE-T1-weighted imaging and 3D selective water excitation, GRE-T1-weighted imaging can be added.

Ankle joint imaging methods

1. Conventional radiography

The standard examination consists of 3 views, the anteroposterior projection, the anteroposterior projection with internal rotation (mortise view), and the lateral view. In the anteroposterior projection, the lateral aspect of the talus and the fibular lateral malleolus are superimposed. However, in the anteroposterior projection with the leg internally rotated 20 degrees, the articular surfaces of the talus, medial malleolus, and lateral malleolus are depicted. The oblique view is also useful for fractures. The dorsiflexion and plantar flexion lateral views and weight-bearing anteroposterior and lateral views are useful for evaluating the articular surface and joint space of the talocrural joint. Stress imaging is performed

to evaluate instability resulting from lateral ligament injury. In anterior drawer radiography, lateral imaging is performed while the subject holds the leg firmly in place with one hand with the ankle in plantar flexion of 20 degrees, grasps the forefoot with the other hand, and pulls it anteriorly. In inversion stress imaging, anteroposterior projection imaging is performed with the foot joint in plantar flexion of approximately 20 degrees and forcibly inverted. The talar tilt angle is then evaluated.

2. Arthrography

Arthrography may be performed for evaluation before and after surgery for osteochondral injury of the trochlea tali. CT or MR arthrography is then subsequently performed. For detailed examination of joint mice, contrast medium and air are injected for double contrast.

3. CT

CT is performed for purposes such as: determining the presence or absence of a fracture difficult to diagnose by conventional radiography, such as bone fragment displacement associated with a fracture or Lisfranc joint injury; determining the presence or absence of loose bodies; osteochondral injury evaluation; and postoperative evaluation. MPR images are generated in 3 planes, transverse, sagittal, and coronal, relative to the articular surface. To enable image reconstruction at high resolution from any angle, the acquired slice thickness specified is the minimum for the system used (≤1 mm). Reconstructed images orthogonal to the target articular surface should be generated for observation using a workstation. A plane orthogonal to the fracture line is useful for diagnosing fracture healing. VR images provide an overall view of fractures and are useful for determining the course of a tendon. If a surgical fixation material is present, the effect of metal artifacts can be reduced by acquiring thin slices, using a soft tissue algorithm for the reconstruction filter, and performing observations with a wide window width. Depending on the CT system used, it may be possible to use metal artifact-reduction technology.

4. MRI

① Body position during imaging and coil used

With the patient in the supine position, the foot is placed in a natural position (normally plantar flexion of approximately 20 degrees), and the ankle joint is held in place with towels or packing material. It is important that the foot position be comfortable to avoid movement artifacts. For the local coil, cylindrical knee coils or head coils are used, as well as ankle coils. If a 2-channel flexible coil is used, it is attached to the medial and lateral sides of the ankle joint.

② Imaging sequences and planes

The imaging sequences and planes vary depending on the target structure. If the target is a ligament or tendon, proton density-weighted, T2-weighted, fat-suppressed T2-weighted, or STIR imaging is performed. If the target is the bone marrow, T1-weighted, fat-suppressed T2-weighted, or STIR imaging is used. For

detailed examination of the articular cartilage, T2-weighted imaging, fat-suppressed, proton density-weighted imaging, 3D, fat-suppressed, GRE-T1-weighted imaging, and 3D GRE with water-selective sequence are useful.

The 3 standard imaging planes for the ankle joint, the sagittal, coronal, and transverse planes, are selected centering on the talocrural joint. Coronal imaging provides good visualization of the ankle mortise and is useful for evaluating the articular surface when the coronal plane is perpendicular to the surface of the distal tibiofibular syndesmosis in transverse imaging at the level of the distal tibiofibular syndesmosis (Fig. 9). If transverse imaging is specified relative to the axis of the lower leg (body axis), the plane may change depending on the degree of ankle plantar flexion. To improve reproducibility, transverse imaging is specified so that it parallels the articular surface of the posterior subtalar joint with the smallest inclination in sagittal imaging (Fig. 10).

Although the imaging parameters vary depending on the MR system, the important recommended parameters are shown in Table 6.

③ Standard imaging methods

(1) Joint sprain

Transverse and coronal imaging: Proton density-weighted and T2-weighted imaging

Sagittal imaging: Fat-suppressed, T2-weighted or STIR imaging

(2) Ankle joint swelling and pain

Sagittal or coronal imaging: T1-weighted, T2-weighted, and fat-suppressed, T2-weighted or STIR imaging

(3) Achilles tendon swelling and pain

The imaging range includes the area from the calcaneal insertion of the Achilles tendon to the muscle tendon junction.

Sagittal imaging: T1-weighted, T2-weighted, and fat-suppressed, T2-weighted or STIR imaging

Transverse imaging: T2-weighted and fat-suppressed, T2-weighted or STIR imaging

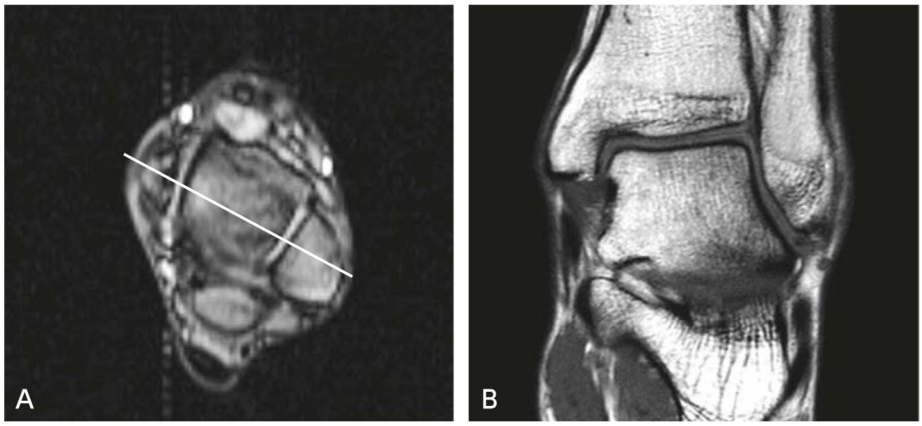

Figure 9. Ankle joint MRI

A: T1-weighted transverse image, B: T1-weighted coronal image

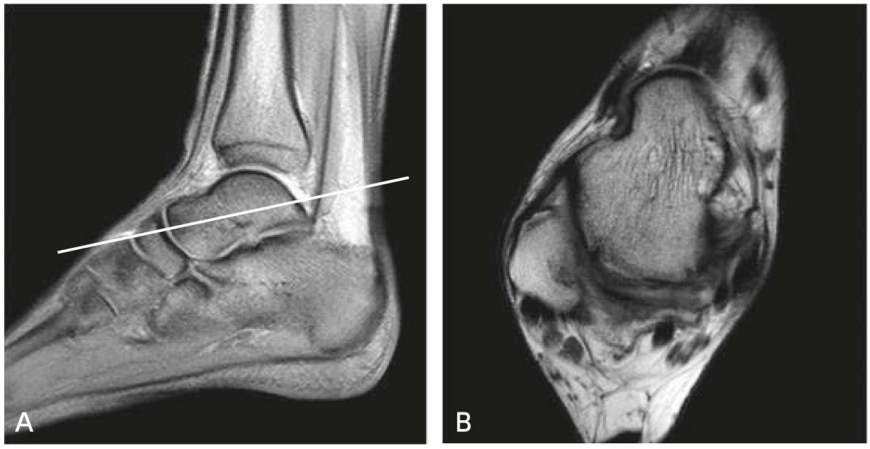

Figure 10. Ankle joint MRI

A: T1-weighted sagittal image, B: T2-weighted oblique transverse image

Table 6 Recommended parameters for MRI

Field of view (FOV)	10 to 15 cm
Slice thickness	3 to 4 mm
Matrix	256 × 204 to 230
Echo train length for proton density-weighted imaging	4 to 6

(4) Plantar pain and swelling

Coronal or sagittal imaging: T1-weighted, T2-weighted, and fat-suppressed, T2-weighted or STIR imaging

(5) Entrapment neuropathy such as plantar numbness

Oblique coronal imaging perpendicular to the posterior subtalar joint: T1-weighted, T2-weighted, and fat-suppressed, T2-weighted or STIR imaging

Sagittal or transverse imaging: Fat-suppressed, T2-weighted or STIR imaging

C Imaging methods for bone and soft tissue tumors and tumor-like lesions

Overview

Conventional radiography provides high diagnostic value in the diagnosis of bone tumors and tumor-like lesions. It should be the first imaging examination performed for this purpose. MRI is excellent for detecting lesions and evaluating local invasion and is often performed following conventional radiography. The modality that plays the central role in the diagnostic imaging of soft tissue neoplasms and tumor-like lesions is MRI, which provides excellent contrast resolution. Conventional radiography is not as useful for diagnosing these lesions as it is for diagnosing bone tumors and tumor-like lesions. However, calcification and ossification patterns in lesions and changes in adjacent bones offer clues for diagnosis. It is therefore useful to perform conventional radiography first. CT is not often aggressively used for tumors or tumor-like lesions in either bone or soft tissue. However, it is suitable for evaluating sites with anatomically complex bone structure and excellent for detecting microscopic ossification and calcification and analyzing the bone cortex in detail.

Detailed discussion

1. Conventional radiography

Conventional radiography is generally performed in the anterior-posterior (frontal) and lateral views (Fig. 11). It is used to analyze the sites and distribution of lesions, their internal and marginal characteristics, and calcified substrates and to evaluate bone cortex changes, periosteal reactions, and soft tissue changes. Imaging from any arbitrary angle can be added as necessary.

2. CT

Thin-section CT is useful for evaluating the bone cortex and ossification/calcification in lesions. Images are acquired with the thinnest possible slice thickness, and MPR images suitable for the evaluation are generated. Thin-section CT is also suitable for detecting small niduses of osteoid osteomas. CT angiography is useful for evaluating vascular anatomy and vascular tumor invasion before and after surgery.

3. MRI

① Body position during imaging and coil used

For the limbs, which are off-center, a body position should be found that places the site being imaged as close to the center of the magnetic field as possible. The optimal coil is selected according to the lesion site and size. For malignancies, the imaging range and coil need to be determined by also taking into account the evaluation of skip lesions and regional lymph nodes. Use of a local coil is appropriate for small subcutaneous lesions of the hands and feet. For tumors of the anterior chest wall, imaging may be performed in the prone position or a bust band used to reduce respiratory artifacts.

② Imaging sequences and planes

SE T1- and T2-weighted imaging is performed to accurately evaluate the internal characteristics of tissue. Fat suppression is used to ① detect adipose tissue, ② improve visualization of edema and inflammation, and ③ increase gadolinium contrast medium enhancement.

The methods of fat-suppressed imaging are: non-selective fat suppression (STIR), which uses the difference in the relaxation times of water and fat; selective fat suppression (chemical shift-selective, CHESS), which uses the difference in the resonance frequencies of water and fat; and water-fat separation (water excitation, Dixon), which uses the difference in the phase dispersions of water and fat. Non-selective and water-fat separation fat-suppression methods are robust against magnetic field non-uniformity and provide stable fat suppression even for sites with complex morphologies, such as the hands and feet. With non-selective fat suppression, tissues with T1 values near that of fat (e.g., hematomas and tissues enhanced by contrast media) are also suppressed. Consequently, contrast-enhanced MRI cannot be used concomitantly. Selective fat suppression involves selectively suppressing only the fat signal by applying frequency-selective excitation pulses that match the resonant frequency of fat protons. It provides good fat suppression. However, it is susceptible to non-uniform fat suppression resulting from magnetic field non-uniformity and therefore requires high static magnetic field uniformity. This limits its imaging range.

With $T2^*$-weighted imaging, magnetic susceptibility is strongly reflected in the images, expanding the signal void. It can therefore sensitively detect hemosiderosis in conditions and lesions such as giant cell tumors of the bone, pigmented villonodular synovitis, and hematomas. Like hemosiderin, ossification/calcification, collagen fibers, and amyloid deposits show hypointensity on T2-weighted imaging. Consequently, $T2^*$-weighted imaging is added when they need to be differentiated from hemosiderin. Diffusion-weighted imaging is a method that emphasizes proton diffusion. In addition to the qualitative diagnosis of lesions including small round cell tumors such as malignant lymphomas, epidermal cysts, and abscesses, it holds promise for preventing the oversight of skip lesions and enlarged lymph nodes.

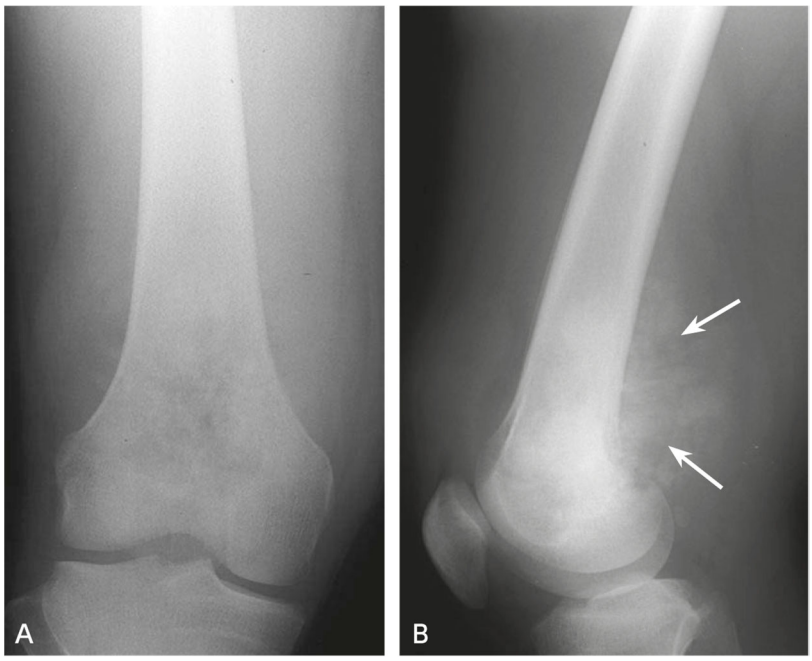

Figure 11. Conventional radiography of osteosarcoma

A: Knee joint, anteroposterior projection; B: Knee joint, lateral view

An osteolytic lesion with indistinct borders is seen in the distal metaphysis of the right femur. Cloud-like calcifications that show bone formation are irregularly mixed in the lesion. In the lateral view, a radial periosteal reaction and soft tissue calcification (→) are seen.

Contrast-enhanced MRI is used for purposes such as differentiating between cystic and solid lesions, identifying appropriate sites for biopsy, determining the presence or absence of inflammatory lesions, and evaluating tumor necrosis after treatment. Dynamic MRI involves rapidly injecting contrast medium intravenously and repeatedly imaging in the same plane. It enables the hemodynamics of tumors to be evaluated and is useful for purposes such as diagnosing highly vascular lesions and distinguishing between residual tumors and post-treatment changes (e.g., edema and fibrosis). MRA can be used to visually identify tumor-associated blood vessels. MRA images can be generated by performing dynamic MRI as a 3D-GRE sequence. They facilitate the visualization of tumor-associated blood vessels and the visual understanding of anatomical spatial relationships.

There are 2 standard imaging planes, along the long and short axes of lesions. In general, transverse and sagittal or transverse and coronal imaging is performed. Transverse imaging is often useful for evaluating invasion of neurovascular bundles in malignancies. The FOV and slice thickness are determined by taking into account the extent of the lesions and the somatotype of the subject. The number of averaged samples and the acquisition matrix are selected so that the SNR is not problematic. The concomitant use of a multichannel coil and parallel imaging can shorten imaging time while maintaining the SNR and is effective when extensive imaging is required.

③ Standard imaging methods

The standard sequences are SE T1- and T2-weighted imaging. Fat suppression should be used concomitantly for at least 1 plane. In addition, diffusion-weighted imaging can be performed in a relatively short time, and its addition is recommended (Fig. 12). The above-mentioned benefits of contrast testing are taken into account in deciding whether it is indicated and whether to perform normal contrast-enhanced MRI or dynamic MRI (Fig. 12). The imaging sequences to be used are determined based on the above considerations. Examples are shown below in Table 7.

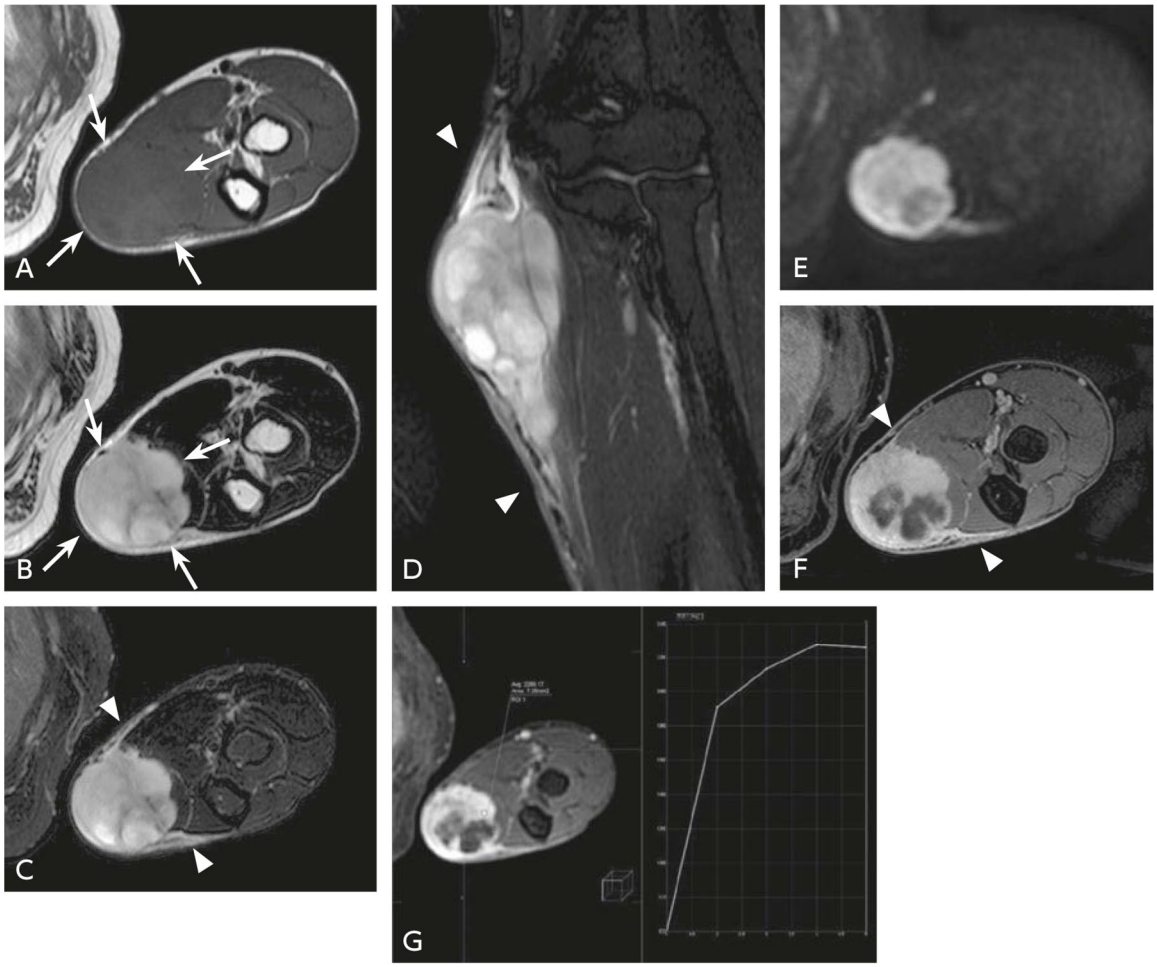

Figure 12. MRI of myxofibrosarcoma

A: T1-weighted transverse image, B: T1-weighted transverse image, C: Fat-suppressed, T2-weighted transverse image, D: Fat-suppressed, T2-weighted sagittal image, E: Diffusion-weighted image (b-value = 1,000 s/mm^2),
F: Fat-suppressed, contrast-enhanced MRI transverse image, G: Dynamic MRI transverse image, optional
A subcutaneous mass with indistinct borders is seen on the medial left upper arm (→). The mass is isointense with muscle in T1-weighted images and shows somewhat non-uniform hyperintensity in T2-weighted images (→). In fat-suppressed, T2-weighted images, hyperintense areas are seen along the fascia transversely and craniocaudally to the tumor (▷). On diffusion-weighted imaging, the mass shows hyperintensity and an ADC value of 1.7×10^{-3} mm/s (ADC map not shown). In the fat-suppressed, contrast-enhanced MRI image, a strongly enhanced solid portion and a weakly enhanced area of degeneration and a necrotic portion are seen. The area along the fascia is also enhanced, and tumor progression (“tail sign”) is seen (▷). Dynamic MRI shows a highly vascular tumor that is enhanced relatively early, which is consistent with findings for myxofibrosarcoma.

4. Nuclear medicine tests

① PET and PET and PET/CT

The radiotracer used for PET is a glucose analog called ^{18}F-FDG. For 2D data acquisition, 185 to 444 MBq (3 to 7 MBq/kg) of FDG are administered intravenously; for 3D data acquisition, 111 to 259 MBq (2 to 5 MBq/kg) are administered. The dose is increased or decreased as appropriate depending on the system used for imaging and the age and body weight of the patient. Sixty to 90 minutes after administration, a PET or PET/CT system is used to perform whole-body emission and transmission scans (in the case of PET) or CT imaging (in the case of PET/CT). In many malignancies, glucose transporter and hexokinase activity are increased, and phosphatase activity is extremely low. Consequently, high levels of FDG accumulate. FDG accumulation in malignancies is also increased more than 1 hour after administration, but it often decreases in benign disease. Consequently, addition of late-phase (2 hours after administration) imaging may aid in distinguishing malignant from benign conditions.

Table 7. Examples of sequences for bone and soft tissue tumors and tumor-like lesions

Imaging Method	Sequence	TR/TE	Other
T2-weighted/transverse	FSE	Approximately ≥ 3,000 ms/100 ms	Imaging slice thickness and FOV changed as appropriate depending on lesion
T1-weighted/transverse	FSE or SE	400 to 750/10 to 12 ms	Imaging slice thickness and FOV changed as appropriate depending on lesion
T2*-weighted (optional)	2D GRE	400 to 600/15 to 20 ms, FA 30°	Added if hemosiderosis suspected
T1-weighted coronal/sagittal	FSE or SE	400 to 750/10 to 12 ms	Imaging slice thickness and FOV changed as appropriate depending on lesion
Fat-suppressed, T2-weighted/ coronal/sagittal	FSE	Approximately ≥ 3,000 ms/100 ms	With the STIR and Dixon methods, good fat suppression is obtained even in areas of magnetic field non-uniformity.
Diffusion-weighted	SE-EPI	5,000 to 6,000/shortest time, ms	b-values of 0 and 1,000 s/mm^2 selected to prepare ADC map
Dynamic MRI (optional)	3D-GRE or 2D-GRE	4 to 5/1.2 to 2 ms or 400/shortest time, ms	Imaging times: 30, 60, 120, and 210 seconds after injection
Gd T1-weighted/transverse, coronal, sagittal	FSE or SE	Approximately 400 to 750/12 ms	Concomitant fat suppression performed for at least 1 angle

② Bone scintigraphy

The radiopharmaceuticals used for bone scintigraphy include ^{99m}Tc-methylene diphosphonate (MDP) and ^{99m}Tc-hydroxymethylene diphosphonate (HMDP). Imaging is performed beginning 2 to 3 hours after intravenous injection and after urination immediately before the test. The use of a low-energy, high-resolution collimator is recommended for the gamma camera used in imaging. Whole-body anterior and posterior views are depicted using a WL setting suitable for bone and soft tissue. If an abnormality is suspected, oblique and expanded acquisition and SPECT or SPECT/CT imaging are performed.

Secondary source materials used as references

1) Uetani M: Diagnostic Imaging of Bone and Soft Tissue, 2nd Edition. Shujunsha, 2010.
2) Fukuda K: MRI of the Joints, 2nd Edition. Medical Science International, 2013.
3) Yamashita Y: Findings of the examination of routine MRI imaging standardization, a research project of the Japanese Society for Magnetic Resonance in Medicine, 1st Report: spine, spinal cord, and mammary gland. Japanese Journal of Magnetic Resonance in Medicine 28: 196-209, 2008.
4) Ross JS et al：Diagnostic imaging spine 1st ed. Amirsys/Elsevier Saunders, 2004
5) Sugimura K: MRI of Bone and Soft Tissue. Medical View, 2000.
6) Schulte-Altedorneburg G: MR arthrography: pharmacology, efficacy and safety in clinical trials. Skeletal Radiol 32: 1-12, 2003
7) Horio S: How to Take and View Plain Radiographs of Bones and Joints, 8th Edition, 2010.
8) Sashi R: MRI of the Shoulder, 2nd Edition. Medical View, 2011.
9) Takahara M et al: Natural progression of osteochondritis dissecans of the humeral capitellum: initial observations. Radiology 216: 207-212, 2000
10) Yanagawa N: Standardization for X-ray CT imaging. Japan Radiological Society, 2010.
11) Timmerman LA et al: Preoperative evaluation of the ulnar collateral ligament by magnetic resonance imaging and computed tomography arthrography: evaluation in 25 baseball players with surgical confirmation. Am J Sports Med 22: 26-31, 1994
12) Uetani M, et al.: Main Points of Bone and Soft Tissue Diagnostic Imaging. Medical View, 2006.
13) Stoller DW: Magnetic resonance imaging in orthopaedics and sports medicine, 3rded. Lippincott Williams & Wilkins, 2007
14) Potter HG et al: High resolution non contrast MRI of the hip. J Magn Reson Imaging 31: 268-278, 2010
15) Niitsu M: Knee MRI, 2nd Edition. Igaku Shoin, 2009.
16) Rogers LF: The ankle, radiology of skeletal trauma 3rded. Churchill Livingstone, 1992
17) Brandser EA et al: contribution of individual projections alone and in combination for radiographic detection of ankle fractures. AJR Am J Roentgenol 174: 1691-1697, 2000
18) Buckwalter KA: Musculoskeletal imaging with multi slice CT. AJR Am J Roentgenol 176: 979-986, 2001
19) Fujimoto H: New Main Points of Bone and Soft Tissue Diagnostic Imaging. Medical View, 2014.
20) Ehara S: Handbook of Bone Trauma Diagnostic Imaging. Medical Science International, 2012.
21) Committee on Bone and Soft Tissue Tumors, Japanese Orthopaedic Association, Ed.: General Rules for Clinical and Pathological Studies on Malignant Bone Tumors, 4th Edition. KANEHARA & Co., 2015.
22) Committee on Bone and Soft Tissue Tumors, Japanese Orthopaedic Association, Ed.: General Rules for Clinical and Pathological Studies on Malignant Soft Tissue Tumors, 3rd Edition. KANEHARA & Co., 2002.
23) Japanese Society of Nuclear Medicine, Ed.: FDG PET and PET/CT Diagnostic Guidelines. Japanese Society of Nuclear Medicine, 2018.
24) Japanese Society of Nuclear Medicine, Ed.: Nuclear Medicine Diagnostic Guidelines. Japanese Society of Nuclear Medicine, 2008.

BQ 78 Is MRI recommended for diagnosing cervical spondylotic myelopathy?

Statement

MRI is useful and recommended for identifying lesion sites, evaluating pathological changes, and predicting prognosis. However, spinal cord compression factors cannot be adequately evaluated with MRI alone. It should therefore be performed in combination with conventional radiography or CT.

Background

MRI has become an essential imaging modality for the diagnosis of cervical spine disease. Its usefulness in diagnosing cervical spondylotic myelopathy was examined.

Explanation

Numerous studies have compared the performance of MRI (Fig.) and other diagnostic imaging modalities in diagnosing cervical spondylotic myelopathy or have examined the correlation between MRI findings and neurological findings or MRI findings and posttreatment prognosis. In an investigation of 26 patients with cervical radiculopathy or cervical myelopathy, Larsson et al. found that MRI together with conventional radiography was suitable as the first line of testing for the diagnosis of cervical spondylotic myelopathy. However, they reported that differentiating between bony and soft tissue spinal cord compression factors was difficult with MRI alone.[1)] Sengupta et al. compared surgical findings and image interpretation results for 41 patients with cervical spondylosis who underwent surgery and also concluded that differentiating between spinal cord compression factors was difficult with MRI.[2)] On the other hand, Nagata et al. analyzed 115 cases of cervical spondylotic myelopathy and found that the severity of spinal cord compression seen on T1-weighted, sagittal MRI images was correlated with myelography findings and clinical severity based on the cervical spondylosis treatment outcome criteria of the Japanese Orthopaedic Association (JOA score).[3)] They therefore concluded that MRI is useful for diagnosis and postoperative evaluation. Bucciero et al. calculated the ratio of the anteroposterior diameter of the spinal cord to the transverse diameter (anteroposterior compression ratio, APCR) in transverse MRI images of 35 patients with cervical spondylotic myelopathy who underwent surgery.[4)] They found that, if the ratio was ≥ 40%, the neurological findings were mild. In patients with a ratio ≥ 10%, the neurological findings indicated a serious condition, and no postoperative improvement was seen. Based on an investigation of 37 patients who underwent surgery, Chung et al. reported that spinal cord compression severity in transverse images was related to postoperative prognosis.[5)] In addition, Wada et al. found that, based on the postoperative outcomes of 50 patients who underwent surgery, the spinal cord cross-sectional area at the site of greatest compression was most highly correlated with prognosis.[6)] Moreover, they found that the area was ≤ 40 mm^2 in many patients whose postoperative improvement rate was poor. Thus, in terms of its ability to directly

visualize spinal cord compression, the usefulness of MRI for diagnosing cervical spondylotic myelopathy, evaluating its pathology, and predicting postoperative prognosis has been demonstrated. However, diagnosis by visual assessment has limitations, particularly the poor interobserver agreement rates that have been reported.[2, 7)]

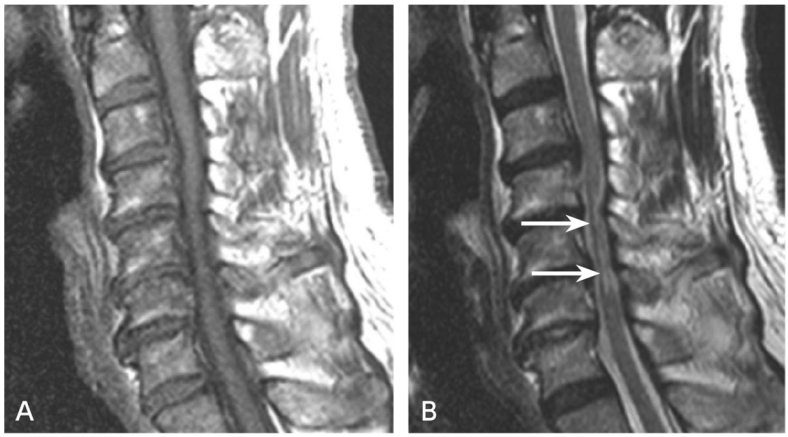

Figure Cervical spondylotic myelopathy

A: MRI, T1-weighted sagittal image; B: MRI, T2-weighted sagittal image
Pronounced intervertebral disc degeneration and proliferative changes in the uncovertebral joints are seen at the C3/4 to C6/7 level. The cervical spinal cord is compressed and flattened, and areas of intraspinal hyperintensity are seen between multiple vertebrae in the T2-weighted image (→).

In cervical spondylotic myelopathy, in addition to morphological changes such as spinal cord compression and flattening, areas of abnormal intraspinal hyperintensity are often seen, particularly on T2-weighted images ("T2 hyperintensity areas" below). This finding is thought to reflect a reversible or irreversible pathological condition.[8)] Although many studies have examined its diagnostic significance, their conclusions have varied. Chung et al. examined 37 patients with cervical spondylotic myelopathy who underwent surgery and reported that T2 hyperintensity areas were not related to postoperative outcome.[5)] Based on an investigation of 52 patients with cervical spondylotic myelopathy who received conservative therapy, Matsumoto et al. concluded that T2 hyperintensity areas were not related to clinical severity or treatment outcome.[9)] However, Chen et al. classified T2 hyperintensity areas as type 1 (indistinct borders with faint hyperintensity) and type 2 (distinct borders with marked hyperintensity) in 64 patients with cervical spondylotic myelopathy who underwent surgery and found that, whereas the prognosis of those with type 1 was similar to that of patients without T2 hyperintensity areas, the prognosis of those with type 2 was poor.[10)] Based on an analysis of the prognosis of 146 patients who underwent surgery, Suri et al. reported that the prognosis was poor if an area of abnormal hyperintensity was seen in T1- or T2-weighted images.[11)] Moreover, in an investigation in 64 patients who underwent surgery, Chatley et al. found that patients with T2 hyperintensity areas in 2 or more vertebral bodies had a poor prognosis.[12)] A similar finding was also described in the report by Wada et al.[6)]

Other studies have examined the diagnostic usefulness of contrast-enhanced MRI. In an investigation of the relationship between preoperative contrast-enhanced, T1-weighted images and clinical symptoms of 683 patients with cervical spondylotic myelopathy who underwent surgery, Ozawa et al. found no significant difference in preoperative JOA scores between a group with intraspinal enhancement and a group without such enhancement.[13] However, postoperative JOA scores were significantly higher in the group without enhancement.

Although MRI is useful for identifying lesion sites, evaluating pathological changes, and predicting prognosis in the diagnosis of cervical spondylotic myelopathy, evaluating spinal cord compression factors with MRI alone is difficult. It should therefore be used in combination with conventional radiography or CT. However, problems remain, such as the fact that the findings lack objectivity (poor interobserver agreement rate) and the fact that no clear conclusion has been reached regarding the significance of T2 hyperintensity areas.

In addition to these typical imaging methods, methods such as diffusion tensor imaging (DTI) are used for diagnosis. To answer the question of whether these methods contribute usefully to early diagnosis and prognosis prediction, further standardization of imaging methods and accumulation of clinical cases are needed.[14] The images normally obtained with MRI are obtained with the patient in the supine position and still, which makes it difficult to evaluate the various dynamic factors involved in spinal cord compression. To solve this problem, the additional use of dynamic/kinetic MRI by means of a device such as an open MRI system has been found to be useful.[15]

Search keywords and secondary sources used as references

PubMed was searched using the following keywords: cervical spondylosis, cervical spondylotic myelopathy, and MRI.

In addition, the following was referenced as a secondary source.

1) The Japanese Orthopaedic Association Clinical Practice Guidelines Committee, Cervical Spondylotic Myelopathy Formulation Committee, Ed.: 2015 Clinical Practice Guidelines for Cervical Spondylotic Myelopathy. Nankodo, 2015.

References

1) Larsson EM et al: Comparison of myelography, CT myelography and magnetic resonance imaging in cervical spondylosis and disk herniation: pre- and postoperative findings. Acta Radiol 30: 233-239, 1989
2) Sengupta DK et al: The value of MR imaging in differentiating between hard and soft cervical disc disease: a comparison with intraoperative findings. Eur Spine J 8: 199-204, 1999
3) Nagata K et al: Clinical value of magnetic resonance imaging for cervical myelopathy. Spine 15: 1088-1096, 1990
4) Bucciero A et al: Cord diameters and their significance in prognostication and decisions about management of cervical spondylotic myelopathy. J Neurosurg Sci 37: 223-228, 1993
5) Chung SS et al: Factors affecting the surgical results of expansive laminoplasty for cervical spondylotic myelopathy. Int Orthop 26: 334-338, 2002
6) Wada E et al: Can intramedullary signal change on magnetic resonance imaging predict surgical outcome in cervical spondylotic myelopathy? Spine 24: 455-461, 1999
7) Cook C et al: Observer agreement of spine stenosis on magnetic resonance imaging analysis of patients with cervical spine myelopathy. J Manipulative Physiol Ther 31: 271-276, 2008

8) Bucciero A et al: MR signal enhancement in cervical spondylotic myelopathy. Correlation with surgical results in 35 cases. J Neurosurg Sci 37: 217-222, 1993
9) Matsumoto M et al: Increased signal intensity of the spinal cord on magnetic resonance images in cervical compressive myelopathy. Does it predict the outcome of conservative treatment? Spine 25: 677-682, 2000
10) Chen CJ et al: Intramedullary high signal intensity on T2-weighted MR images in cervical spondylotic myelopathy: prediction of prognosis with type of intensity. Radiology 221: 789-794, 2001
11) Suri A et al: Effect of intramedullary signal changes on the surgical outcome of patients with cervical spondylotic myelopathy. Spine 3: 33-45, 2003
12) Chatley A et al: Effect of spinal cord signal intensity changes on clinical outcome after surgery for cervical spondylotic myelopathy. J Neurosurg Spine 11: 562-567, 2009
13) Ozawa H et al: Clinical significance of intramedullary Gd-DTPA enhancement in cervical myelopathy. Spinal Cord 48: 415-422, 2010
14) Martin AR et al: Translating state-of-the-art spinal cord MRI techniques to clinical use: a systematic review of clinical studies utilizing DTI, MT, MWF, MRS, and fMRI. Neuroimage Clin 10: 192-238, 2015
15) Kolcun JP, et al: The role of dynamic magnetic resonance imaging in cervical spondylotic myelopathy. Asian Spine J 11: 1008-1015, 2017

BQ 79 Is MRI recommended for diagnosing lumbar disc herniation?

Statement

Non-contrast MRI is useful and recommended for diagnosing lumbar disc herniation. Contrast-enhanced MRI may be useful for the follow-up of intervertebral disc herniation, differentiation from tumors, and diagnosis of postoperative recurrence. Consequently, its use can be considered. There is no scientific evidence that MR myelography should be used in addition to non-contrast MRI, and its use is therefore not recommended.

Background

MRI is minimally invasive and results in no radiation exposure, and it has become an essential diagnostic imaging modality for diagnosing lumbar spine disease. The usefulness of plain and contrast-enhanced MRI and MR myelography in diagnosing lumbar disc herniation was examined.

Explanation

Studies have compared the performance of non-contrast MRI (Fig.) and other diagnostic imaging modalities in diagnosing lumbar disc herniation. Janssen et al. compared non-contrast MRI, myelography, and CT myelography in 60 patients who underwent surgery for suspected intervertebral disc herniation and found that the diagnostic accuracy rate was 96% for non-contrast MRI, 81% for myelography, 57% for CT myelography, and 84% for the combination of myelography and CT myelography.[1)] Thus, the diagnostic accuracy rate was the highest with non-contrast MRI. On the other hand, Thornbury et al. compared non-contrast MRI, CT, and CT myelography in 95 patients with lumbar pain (56 underwent surgery) and found no significant differences in their diagnostic performance.[2)] Szypryt et al. compared non-contrast MRI and myelography in 30 patients who underwent surgery for suspected intervertebral disc herniation and found that the diagnostic accuracy rate was 88% for non-contrast MRI and 75% for myelography. Thus, non-contrast MRI was found to be slightly superior.[3)] The fact that non-contrast MRI shows diagnostic performance comparable or superior to that of other diagnostic imaging modalities, combined with the fact that it results in no radiation exposure and is minimally invasive, makes it the most highly recommended modality.

With regard to the usefulness of non-contrast MRI in evaluating radiculopathy, studies have examined the relationship between nerve root sheath morphology, compression severity, and intervertebral disc herniation. Gorbachova et al. examined non-contrast MRI in 96 patients and reported finding no relationship between the short-axis diameter of the nerve root sheath and the presence or absence of intervertebral disc herniation.[4)] On the other hand, Pfirrmann et al. found that the severity of nerve root compression (4-step classification) resulting from intervertebral disc herniation was well correlated with non-contrast MRI and intraoperative findings for 94 nerve roots examined by surgery.[5)] Although there have been studies showing correlations between leg pain and the severity of nerve root compression and

intervertebral disc herniation, no studies have showed consistency between pain sites and non-contrast MRI findings.[6, 7] In a recent study, Mostofi et al. examined the medical records of 241 patients diagnosed with lumbar disc herniation and found that 27 of these patients (11.20%) had hernia findings on the symptomatic side and contralateral side.[8]

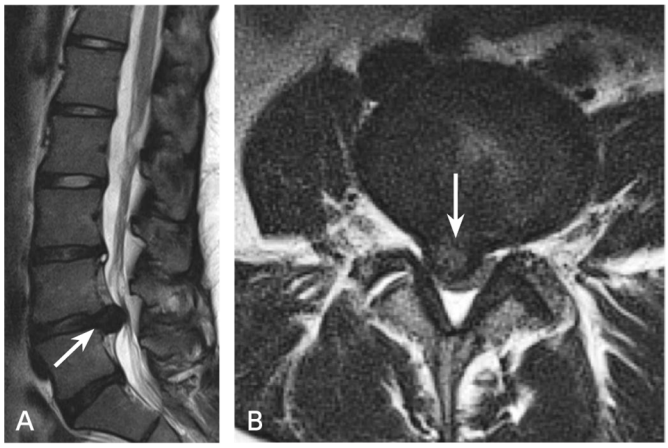

Figure. Lumbar disc herniation

A: MRI, T2-weighted sagittal image; B: MRI, T2-weighted transverse image, L4/5 level Herniation of the intervertebral disc at the L4/5 level is seen extruding posteriorly and slightly to the right (→), resulting in spinal canal stenosis.

Some studies have shown contrast MRI to be useful for the follow-up of intervertebral disc herniation. Komori et al. examined the contrast-enhanced MRI images of 48 patients with unilateral nerve root symptoms and reported that intervertebral disc herniation that showed ring-shaped contrast enhancement was susceptible to resorption.[9] Autio et al. examined the contrast-enhanced MRI images of 160 patients with unilateral sciatic neuralgia and found that thick ring-shaped enhancement of an intervertebral disc herniation, a higher degree of herniation displacement, and being aged 41 to 50 years were related to the hernia resorption rate.[10] Although the findings of detached intervertebral disc herniation are often confusingly similar to tumor findings, contrast-enhanced MRI has been reported to be useful for distinguishing such hernias from tumors.[11, 12] In addition, Hueftle et al. compared the MRI and pathological findings of 17 patients with failed back surgery syndrome who underwent surgery and found that early contrast-enhanced MRI images, obtained within 10 minutes after contrast administration, were useful for differentiating between epidural fibrosis and the recurrence of intervertebral disc herniation.[13] Amador et al. performed contrast-enhanced MRI in 72 patients diagnosed with intervertebral disc herniation by CT performed for acute lumbar sciatic neuralgia and examined whether the presence or absence of contrast enhancement was useful for predicting hernia disappearance 1 year later. Although hernias without contrast enhancement tended to remain, no significant correlation was seen between the contrast pattern and hernia disappearance.[14] Contrast-enhanced MRI is normally not needed to diagnose intervertebral disc herniation. However, it may be useful for follow-up, differentiating from tumors, and diagnosing postoperative recurrence.

MR myelography is excellent for visualizing the subarachnoid space and nerve root and ganglion morphology and is used as a substitute for myelography. Aota et al. examined 83 patients diagnosed with intervertebral disc herniation by MRI and found that swelling and deformation of the nerve roots and dorsal root ganglia were distinctly visualized, and that the severity of these changes and leg pain severity were well correlated.[15] On the other hand, Pui et al. examined 72 patients diagnosed with intervertebral disc herniation of the cervical or lumbar spine by MRI and found that adding MR myelography to non-contrast MRI did not improve diagnostic performance with respect to hernias.[16] O'Connell et al. examined 207 patients with lumbar pain or spinal radicular symptoms and concluded that adding MR myelography to non-contrast MRI did not yield much additional information.[17] Wilmink concluded that, although MR myelography is useful for elucidating the relationship between sciatic neuralgia and the appearance of nerve root compression caused by a change such as intervertebral disc herniation, it is not an imaging method that can replace non-contrast MRI.[18] Based on these findings, there is no evidence indicating that MR myelography should be added to non-contrast MRI, and the use of MR myelography is therefore not recommended.

Search keywords and secondary sources used as references

PubMed was searched using the following keywords: back pain, sciatica, disk herniation, and MRI.

In addition, the following was referenced as a secondary source.

1) Japanese Orthopaedic Association and Japanese Society for Spine Surgery and Related Research, Ed.: Clinical Practice Guidelines for Lumbar Disc Herniation, Revised 2nd Edition. Nankodo Co., 2011.

References

1) Janssen ME et al: Lumbar herniated disk disease: comparison of MRI, myelography, and post-myelographic CT scan with surgical findings. Orthopedics 17: 121-127, 1994
2) Thornbury JR et al: Disk-caused nerve compression in patients with acute low-back pain: diagnosis with MR, CT myelography, and plain CT. Radiology 186: 731-738, 1993
3) Szypryt EP et al: Diagnosis of lumbar disc protrusion: a comparison between magnetic resonance imaging and radiculography. J Bone Joint Surg Br 70: 717-722, 1988
4) Gorbachova TA et al: Nerve root sleeve diameters at normal segments and at segments with proximate disc disease: MRI evaluation. Skeletal Radiol 31: 511-515, 2002
5) Pfirrmann CWA et al: MR image-based grading of lumbar nerve root compromise due to disk herniation: reliability study with surgical correlation. Radiology 230: 583-588, 2004
6) Porchet F et al: Relationship between severity of lumbar disc disease and disability scores in sciatica patients. Neurosurgery 50: 1253-1259, 2002
7) Beattie PF et al: Associations between patient report of symptoms and anatomic impairment visible on lumbar magnetic resonance imaging. Spine 25: 819-828, 2000
8) Mostofi K et al: Reliability of the path of the sciatic nerve, congruence between patients' history and medical imaging evidence of disc herniation and its role in surgical decision making. Asian Spine J 9: 200-204, 2015
9) Komori H et al: Contrast-enhanced magnetic resonance imaging in conservative management of lumbar disc herniation. Spine 23: 67-73, 1998
10) Autio RA et al: Determinants of spontaneous resorption of intervertebral disc herniations. Spine 31: 1247-1252, 2006
11) Aydin MV et al: Intradural disc mimicking: a spinal tumor lesion. Spinal Cord 42: 52-54, 2004
12) Lee JS et al: Intradural disc herniation at L5-S1 mimicking an intradural extramedullary spinal tumor: a case report. J Korean Med Sci 21: 778-780, 2006
13) Hueftle MG et al: Lumbar spine: postoperative MR imaging with Gd-DTPA. Radiology 167: 817-824, 1988

14) Amador AR et al: Natural history of lumbar disc hernias: does gadolinium enhancement have any prognostic value ? Radiologia 55: 398-407, 2013
15) Aota Y et al: Dorsal root ganglia morphologic features in patients with herniation of the nucleus pulposus. Spine 26: 2125- 2132, 2001
16) Pui MH et al: Value of magnetic resonance myelography in the diagnosis of disc herniation and spinal stenosis. Australas Radiol 44: 281-284, 2000
17) O'Connell MJ et al: The value of routine MR myelography at MRI of the lumbar spine. Acta Radiol 44: 665-672, 2003
18) Wilmink JT: MR myelography in patients with lumbosacral radicular pain: diagnostic value and technique. Neuroradiol J 24: 570-576, 2011

BQ 80 Is hand and wrist joint MRI recommended for diagnosing rheumatoid arthritis (RA)?

Statement

Hand and wrist joint MRI is useful and recommended. It is preferably used in combination with contrast-enhanced imaging and should be performed together with an examination by a rheumatologist and serological testing.

Background

The findings of joint MRI in RA include synovial thickening, bone marrow edema, bone erosion, synovial fluid accumulation, and tenosynovitis. However, the specificity of these findings is weak, and similar findings may be obtained in other inflammatory joint diseases. The 2010-ACR/EULAR criteria emphasize the distribution of subjective and objective findings such as joint pain and swelling and the number of affected joints (secondary source 1) and do not include items related to joint MRI. The usefulness of hand and wrist joint MRI in diagnosing RA was examined.

Explanation

Why is hand and wrist MRI a subject of debate even though RA is a systemic disorder that affects a variety of joints and organs? One answer is that the hand and wrist joints are sites where RA occurs preferentially, and bone erosion can be more easily observed in these joints than in larger joints.[1)] In addition, the changes that occur in joints throughout the body can to a certain extent be understood by evaluating the hand and wrist joints, according to an investigation of whole-body MRI.[2)]

The standard imaging methods used are T1-weighted, fat-suppressed, T2-weighted (or STIR imaging), and post-contrast, fat-suppressed, T1-weighted imaging. Contrast-enhanced imaging is not always essential for evaluating bone erosion and bone marrow edema. However, the use of fat-suppressed, T2-weighted imaging (or STIR imaging) to evaluate synovitis and tenosynovitis can result in underestimation or overestimation, and contrast-enhanced imaging is therefore essential for their accurate evaluation.[3, 4)] Imaging of both hands is preferable if possible.[5)]

Several cohort studies have examined the usefulness of hand and wrist joint MRI (Fig.) in diagnosing RA. Some studies have found hand and wrist joint MRI to not be useful for distinguishing between early RA and other inflammatory joint diseases.[6, 7)] On the other hand, Sugimoto et al. found that, in 48 patients with suspected early RA, supplementing the 1987-ACR criteria with MRI diagnostic criteria (secondary source 2, bilateral hand joints, metacarpophalangeal joint, and proximal interphalangeal joint contrast enhancement) improved the diagnostic sensitivity and accuracy rates, with the rates of diagnostic sensitivity, specificity, and accuracy changing from 77%, 91%, and 83%, respectively, to 96%, 86%, and 94%, respectively.[8)] In an investigation of MRI of the bilateral hand joints and serum markers in 129 patients

with unclassified arthritis, Tamai et al. found that the combination of bone marrow edema visualized by MRI and anti-CCP antibody positivity was useful for diagnosing RA.[9)]

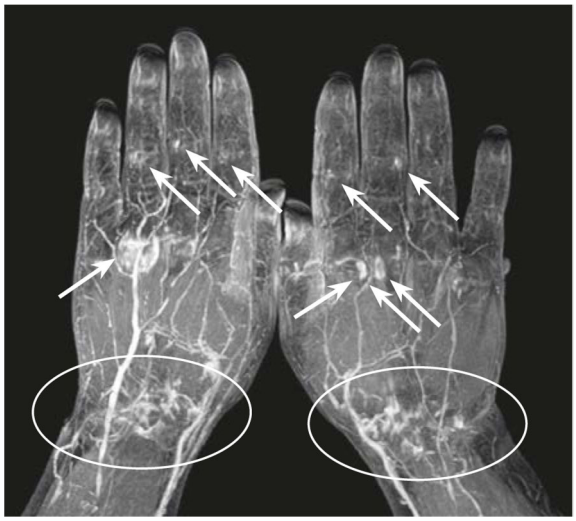

Figure RA

MRI of both hands, fat-suppressed, contrast-enhanced, T1-weighted imaging, MIP image: Multiple areas of abnormal enhancement are seen in the bilateral carpal regions (circled areas) and finger joints (→), findings indicative of polyarthritis.

According to a meta-analysis by Suter et al., the diagnostic performance of hand and wrist joint MRI in early RA varies greatly depending on the MRI diagnostic criteria used, with sensitivity ranging from 20% to 100% and specificity from 0% to 100%.[10)] Although it is difficult to characterize the diagnostic performance of hand and wrist MRI based on those results, an examination of the details shows that sensitivity and specificity were relatively high for the combination of synovitis, bone marrow edema, and bone erosion, and that specificity tended to be high and sensitivity low only for bone marrow edema and bone erosion. Hand and wrist joint MRI should therefore be used in combination with contrast-enhanced imaging to visualize synovitis. Moreover, specificity can be improved by keeping in mind that a few arthritis findings can be observed even in healthy individuals, particularly elderly individuals.[11)]

For the diagnosis of RA, hand and wrist joint MRI is preferably performed in combination with contrast-enhanced imaging, and interpretation should take into account the normal ranges for findings. Moreover, rather than a diagnosis based on MRI alone, an evaluation that combines MRI with an examination by a rheumatologist and serological testing is recommended.

Search keywords and secondary sources used as references

PubMed was searched using the following keywords: hand, wrist, rheumatoid arthritis, diagnosis, and MRI.

In addition, the following were referenced as secondary sources.

1) Aletaha D et al: 2010 Rheumatoid arthritis classification criteria: an American College of Rheumatology/European League Against Rheumatism collaborative initiative. Arthritis Rheum 62 (9): 2569-2581, 2010
2) Arnet FC et al: The American Rheumatism Association 1987 revised criteria for the classification of rheumatoid arthritis. Arthritis Rheum 31: 315-324, 1988

References

1) Rubin DA: MRI and ultrasound of the hands and wrists in rheumatoid arthritis: imaging findings. Skeletal Radiol 48 (5): 677-695, 2019
2) Kamishima T et al: Contrast-enhanced whole-body joint MRI in patients with unclassified arthritis who develop early rheumatoid arthritis within 2 years: feasibility study and correlation with MRI findings of the hands. AJR Am J Roentgenol 195 (4): W287-W292, 2010
3) Stomp W et al: Aiming for a simpler early arthritis MRI protocol: can Gd contrast administration be eliminated? Eur Radiol 25 (5): 1520-1527, 2015
4) Aoki T et al: Diagnosis of early-stage rheumatoid arthritis: usefulness of unenhanced and gadolinium-enhanced MR images at 3T. Clin Imaging 37 (2): 348-353, 2013
5) Mo YQ et al: Magnetic resonance imaging of bilateral hands is more optimal than MRI of unilateral hands for rheumatoid arthritis. J Rheumatol 45 (7): 895-904, 2018
6) Boutry N et al: MR imaging findings in hands in early rheumatoid arthritis: comparison with those in systemic lupus erythematosus and primary Sjogren syndrome. Radiology 236 (2): 593-600, 2005
7) Duer-Jensen A et al: Bone edema on magnetic resonance imaging is an independent predictor of rheumatoid arthritis development in patients with early undifferentiated arthritis. Arthritis Rheum 63 (8): 2192-2202, 2011
8) Sugimoto H et al: Early-stage rheumatoid arthritis: prospective study of the effectiveness of MR imaging for diagnosis. Radiology 216 (2): 569-575, 2000
9) Tamai M et al: A prediction rule for disease outcome in patients with undifferentiated arthritis using magnetic resonance imaging of the wrists and finger joints and serologic autoantibodies. Arthritis Rheum 61 (6): 772-778, 2009
10) Suter LG ey al: Role of magnetic resonance imaging in the diagnosis and prognosis of rheumatoid arthritis. Arthritis Care Res (Hoboken) 63 (5): 675-688, 2011
11) Boer AC et al: Using a reference when defining an abnormal MRI reduces false-positive MRI results-a longitudinal study in two cohorts at risk for rheumatoid arthritis. Rheumatology 56 (10): 1700-1706, 2017

CQ 19 Is MR arthrography recommended for diagnosing rotator cuff injury?

Recommendation

Although there are reports indicating that the diagnostic performance of MR arthrography in evaluating subscapularis tendon rupture and the postoperative shoulder rotator cuff is superior to that of non-contrast MRI, nearly all of the reports as a whole indicate that the sensitivity and specificity of MR arthrography and non-contrast MRI are comparable in the diagnosis of rotator cuff injury. It is therefore weakly recommended that MR arthrography not be performed in view of its invasiveness.

Recommendation strength: 3, strength of evidence: weak (C), agreement rate: 100% (9/9)

Background

MRI is known to be useful for diagnosing rotator cuff injury. However, whether MR arthrography, which is invasive, is necessary for diagnosis is not yet known. Consequently, the need for MR arthrography was examined.

Explanation

There have been 6 meta-analysis articles[1-6] and 2 articles[7, 8] describing cross-sectional studies of the diagnostic performance of MRI, including MR arthrography and non-contrast MRI, in rotator cuff injury. A systematic review of these articles was conducted. The sensitivity and specificity reported were as follows. The sensitivity and specificity of non-contrast MRI ranged from 77% to 96% and from 81% to 100%, respectively.[1-6] The sensitivity and specificity of MR arthrography ranged from 77% to 100% and from 92% to 100%, respectively.[1-6] These results indicate that the diagnostic performance of MR arthrography and non-contrast MRI is comparable.

A systematic review by Lenza et al. found that sensitivity and specificity in the diagnosis of full-thickness (complete) rotator cuff tear were 94% and 93%, respectively, for non-contrast MRI and 94% and 92%, respectively, for MR arthrography.[1] No statistically significant differences were seen. In a meta-analysis by de Jesus et al., sensitivity and specificity in the diagnosis of partial and full-thickness rotator cuff tears were 87.0% and 81.7%, respectively, for non-contrast MRI (Fig. A) and 92.3% and 94.5%, respectively, for MR arthrography (Fig. B).[2] The area under the curve (AUC) in the ROC analysis was 0.935 for MR arthrography and 0.878 for non-contrast MRI. In a meta-analysis by Dinnes et al., sensitivity and specificity in the diagnosis of full-thickness tears were 89% and 93%, respectively, for non-contrast MRI and 95% and 93%, respectively, for MR arthrography.[3] However, the diagnostic performance of both was low for partial (incomplete) tears.

In a meta-analysis by McGarvey et al. of studies that used recent MRI systems that were limited exclusively to 3T-MRI, sensitivity and specificity for full-thickness tears were 95.7% and 99.0%,

respectively, for non-contrast MRI and 96.5% and 97.8%, respectively, for MR arthrography.[4] Thus, the diagnostic performance of the 2 methods was comparable. However, sensitivity and specificity for diagnostic performance in partial tears were 80.5% and 100%, respectively, for non-contrast MRI versus 86.5% and 95.2%, respectively, for MR arthrography, indicating that MR arthrography was more sensitive than non-contrast MRI, and non-contrast MRI was more specific than MR arthrography, the differences being significant. With regard to diagnostic performance in subscapularis tendon rupture, that of MR arthrography tends to be superior to that of non-contrast MRI overall. In a meta-analysis by Huang et al. of diagnostic performance in partial bursal surface tears, the sensitivity, specificity, and AUC were 77%, 96%, and 0.82, respectively, for non-contrast MRI and 77%, 98%, and 0.88, respectively, for MR arthrography, indicating that the diagnostic performance of the 2 methods was comparable.[5] With regard to diagnostic performance in rotator cuff tears, Roy et al. reported that sensitivity and specificity were both 90% with both non-contrast MRI and MR arthrography, indicating comparable diagnostic performance for both.[6]

For rotator cuff tear evaluation in the postoperative shoulder, Magee et al. reported sensitivity and specificity of 84% and 100%, respectively, with non-contrast MRI and 100% and 100%, respectively, with MR arthrography.[7, 8] Thus, the diagnostic performance of MR arthrography was higher.

The above findings indicate that, although some reports show that MR arthrography provides superior diagnostic performance in subscapularis tendon injury and postoperative rotator cuff tear, nearly all of the reports indicate that the performance of non-contrast MRI and MR arthrography is basically comparable in the diagnosis of rotator cuff injury. Although there were no reports of adverse reactions to contrast media with MR arthrography, it is weakly recommended that MR arthrography not be performed in view of its invasiveness.

Figure　Rotator cuff tear

A: MRI of a full-thickness rotator cuff tear, fat-suppressed, proton density-weighted, oblique coronal image: A continuous interruption and defect are seen through the full thickness of the superior rotator cuff (→). The glenohumeral joint and subacromial bursa communicate through this site.

B: MR arthrography of a partial rotator cuff tear, fat-suppressed, T1-weighted, oblique coronal image: Contrast medium influx is seen on the articular surface at the greater tubercle insertion of the superior rotator cuff (→).

Search keywords and secondary sources used as references

PubMed, the Ichushi, and Cochrane Library databases were searched using the following keywords: rotator cuff injury, rotator cuff tear, MRI, MR arthrography, humans, human, sensitivity, specificity, and ROC. The period searched was from January 2016 to July 2020, and hits were obtained for 110 articles. Two articles were extracted in the secondary screening. In addition, 3 articles were added with a hand search. A qualitative systematic review of these articles was conducted.

In addition, the following was referenced as a secondary source.

1) Japan Radiological Society, Ed.: Diagnostic Imaging Guidelines 2016. KANEHARA & Co., 2016.

References

1) Lenza M et al: Magnetic resonance imaging, magnetic resonance arthrography and ultrasonography for assessing rotator cuff tears in people with shoulder pain for whom surgery is being considered. Cochrane Detabase Syst Rev 24: 9, 2013
2) de Jesus JO et al: Accuracy of MRI, MR arthrography, and ultrasound in the diagnosis of rotator cuff tears: a meta-analysis. AJR Am J Roentgenol 192: 1701-1707, 2009
3) Dinnes J et al: The effectiveness of diagnostic tests for the assessment of shoulder pain due to soft tissue disorders: a systematic review. Health Technol Assess 7: 1-166, 2003
4) McGarvey C et al: Diagnosis of rotator cuff tears using 3-tesla MRI versus 3-tesla MRA: a systematic review and meta-analysis. Skeletal Radiol 45 (2): 251-261, 2016
5) Huang T et al: Diagnostic accuracy of MRA and MRI for the bursal-sided partial-thickness rotator cuff tears: a meta-analysis. J Orthop Surg Res 14 (1): 436, 2019
6) Roy JS et al: Diagnostic accuracy of ultrasonography, MRI and MR arthrography in the characterisation of rotator cuff disorders: a systematic review and meta-analysis. Br J Sports Med 49 (20): 1316-1328, 2015
7) Magee T: Imaging of the post-operative shoulder: does injection of iodinated contrast in addition to MR contrast during arthrography improve diagnostic accuracy and patient throughput? Skeletal Radiol 47 (9): 1253-1261, 2018
8) Magee T: Utility of pre- and post-MR arthrogram imaging of the shoulder: effect on patient care. Br J Radiol 89 (1062): 20160028, 2016

CQ 20 Is MR arthrography recommended for diagnosing a glenoid labrum tear?

Recommendation

MR arthrography is weakly recommended for diagnosing a glenoid labrum tear.

Recommendation strength: 2, strength of evidence: weak (C), agreement rate: 89% (8/9)

Background

MRI is a widely used and useful test for diagnosing shoulder joint diseases, and the use of non-contrast MRI for this purpose is recommended. MR arthrography includes direct MR arthrography, in which observations are performed after a contrast medium is administered in the joint and the joint capsule has been relaxed, and indirect MR arthrography, in which a contrast medium is administered intravenously. Although there is evidence suggesting that MR arthrography may provide higher diagnostic performance than non-contrast MRI for glenoid labrum lesions, its use is not uniformly recommended. This CQ discusses the usefulness of MR arthrography in diagnosing glenoid labrum tears.

Explanation

There have been 1 cohort study,[1)] 2 cross-sectional studies,[2, 3)] and 3 meta-analyses[4-6)] that examined the diagnostic performance of MR arthrography and non-contrast MRI in glenoid labrum tear, using shoulder arthroscopy as the reference standard. A qualitative systematic review of the articles describing these studies was conducted. Three types of glenoid labrum injuries (superior labrum anterior and posterior (SLAP) lesions[1-6)], anterior glenoid labrum lesions[2-4)], and posterior glenoid labrum lesions) were evaluated respectively[2-4)]

Aspects of the studies, such as the magnetic fields of the MRI systems used and the patient groups examined, varied. In particular, variability in the diagnostic performance of non-contrast MRI was seen with low magnetic field systems and 3T-MRI. Nearly all of the reports showed that MR arthrography provided better sensitivity for all of these types of glenoid labrum tears (MR arthrography, 80% to 100%; non-contrast MRI, 23% to 98%), whereas the specificity of the 2 methods was roughly comparable (MR arthrography, 81% to 100%; non-contrast MRI, 88% to 100%).[1-6)]

In studies that compared the diagnostic performance of direct and indirect MR arthrography with that of non-contrast MRI in SLAP lesions, sensitivity ranged from 80.4% to 85% with direct MR arthrography, 74.2% to 78% with indirect MR arthrography, and 63% to 83% with non-contrast MRI, whereas specificity ranged from 90.7% to 94%, 61% to 66.5%, and 87.2% to 99%, respectively.[4, 5)] Thus, the diagnostic performance of indirect MR arthrography was inferior with respect to both sensitivity and specificity. This is likely attributable in large part to factors such as inadequate expansion of the joint capsule and interpretation interference by soft tissue contrast enhancement with indirect MR arthrography.

Figure 1. SLAP lesion

MRI, fat-suppressed, T2-weighted, oblique coronal image: A hyperintense region is seen at the attachment of the superior glenoid labrum (→).

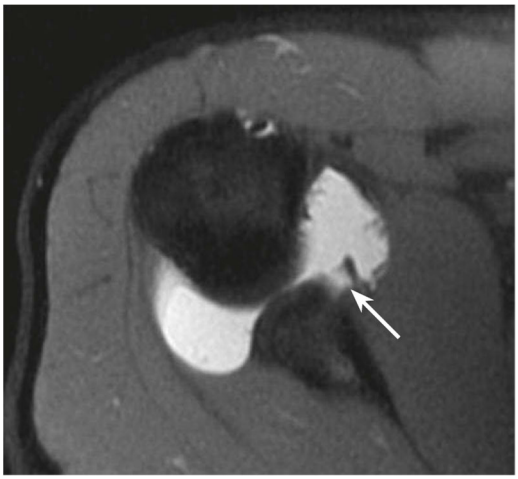

Figure 2. Anterior glenoid labrum detachment resulting from anterior shoulder dislocation (Bankart lesion)

Direct MR arthrography, fat-suppressed, T1-weighted, transverse image: Contrast medium influx is seen near the inner border of the anterior glenoid labrum (→).

With regard to abduction and external rotation (ABER), sensitivity and specificity for anterior glenoid labrum tear were 83% and 99%, respectively, with non-contrast MRI, 87% and 99%, respectively, with MR arthrography (regardless of whether it was contrast-enhanced imaging), and 94% and 94%, respectively, with MR arthrography in ABER. Sensitivity and specificity for SLAP lesions were 83% and 99%, respectively, with non-contrast MRI, 84% and 92%, respectively, with MR arthrography (regardless of whether it was contrast-enhanced imaging), and 100% and 100%, respectively, with MR arthrography in ABER.[4)] Thus, sensitivity improved with ABER. With regard to diagnostic performance improvements resulting from the addition of ABER, it should be noted that it was not always added in the reports that were examined, and that it was added only for patients in whom instability was seen clinically in some of the included reports.

In the postoperative shoulder, symptoms suggestive of recurrence are seen in approximately 20% of patients, and differentiation of the glenoid labrum that has undergone postoperative changes and recurrence is difficult. Magee compared sensitivity and specificity in the postoperative shoulder and reported sensitivity and specificity for SLAP lesions of 100% and 97%, respectively, with MR arthrography and 71% and 100%, respectively, with non-contrast MRI. For the anterior glenoid labrum lesion, sensitivity and specificity were 100% and 100%, respectively, with MR arthrography and 80% and 100%, respectively, with non-contrast MRI. For the posterior glenoid labrum, sensitivity and specificity were 100% and 98%, respectively, with MR arthrography and 81% and 100%, respectively, with non-contrast MRI.[2)] Thus, MR arthrography was found to be useful. However, 22 patients in this study who could not be evaluated by MR arthrography or non-contrast MRI due to metal artifacts were instead evaluated by CT arthrography and

excluded from the analysis. It should be noted that this was considered to result in sensitivity and specificity that were higher than those in the previous studies.

In a study that evaluated the effectiveness of MR arthrography in patient care, the sensitivity of MR arthrography and non-contrast MRI was 96% to 98% and 81% to 83%, respectively, for SLAP lesions, 94% to 97% and 74% to 77%, respectively, for anterior glenoid labrum lesions, and 91% to 97% and 76% to 82%, respectively, for posterior glenoid labrum lesions, showing that MR arthrography is superior to non-contrast MRI. The specificity of MR arthrography and non-contrast MRI was 100% for all 3 types of lesions.[3)] Abnormalities were seen by MR arthrography in 18 of the 48 patients (37%) with normal findings on non-contrast MRI, and additional findings were obtained by MR arthrography in only 3 of the 42 patients (6%) with abnormalities seen on non-contrast MRI. These additional findings were lesions that were clinically identifiable by arthroscopy, suggesting that additional MR arthrography may not be necessary for patients with abnormalities seen on non-contrast MRI.

MR arthrography, particularly direct MR arthrography, is invasive and time-consuming and has problems such as patient discomfort before and after the procedure, risk of infection, and cost. However, there is weak evidence that it is superior to non-contrast MRI for evaluating glenoid labrum tears, and its use is therefore weakly recommended.

Search keywords and secondary sources used as references

PubMed was searched using the following keywords: shoulder, labrum, labral, injury, tear, MR arthrography, MRI, humans, human, sensitivity, specificity, and ROC. The period searched was from January 2016 to July 2020; hits were obtained for 40 articles. The Ichushi and Cochrane Library databases were also searched using the same keywords. Six articles were extracted in the secondary screening, and a qualitative systematic review of the articles was conducted.

In addition, the following was referenced as a secondary source.

1) Japan Radiological Society, Ed.: Diagnostic Imaging Guidelines 2016. KANEHARA & Co., 2016.

References

1) Berth A et al: Magnetic resonance-guided direct shoulder arthrography for the detection of superior labrum anterior-posterior lesions using an open 1.0-T MRI scanner. Pol J Radiol 84: e251-e257, 2019
2) Magee T: Imaging of the post-operative shoulder: does injection of iodinated contrast in addition to MR contrast during arthrography improve diagnostic accuracy and patient throughput? Skeletal Radiol 47 (9): 1253-1261, 2018
3) Magee T: Utility of pre- and post-MR arthrogram imaging of the shoulder: effect on patient care. Br J Radiol 89 (1062): 20160028, 2016
4) Ajuied A et al: Diagnosis of glenoid labral tears using 3-tesla MRI vs. 3-tesla MRA: a systematic review and meta-analysis. Arch Orthop Trauma Surg 138 (5): 699-709, 2018
5) Symanski JS et al: Diagnosis of superior labrum anterior-to-posterior tears by using MR imaging and MR arthrography: a systematic review and meta-analysis. Radiology 285 (1): 101-113, 2017
6) Arirachakaran A et al: A systematic review and meta-analysis of diagnostic test of MRA versus MRI for detection superior labrum anterior to posterior lesions type II-VII. Skeletal Radiol 46 (2): 149-160, 2017

BQ 81 Are conventional radiography, bone scintigraphy, and MRI recommended for diagnosing idiopathic osteonecrosis of the femoral head?

Statement

Conventional radiography, bone scintigraphy, and MRI are standard imaging examinations included among the diagnostic criteria and staging and disease classification of the working group of the Specific Disease Investigation Committee under the auspices of the Japanese Ministry of Health, Labour and Welfare of idiopathic osteonecrosis of the femoral head, and their use for diagnosing idiopathic osteonecrosis of the femoral head is recommended.

CQ 21 Is CT recommended for diagnosing idiopathic osteonecrosis of the femoral head?

Recommendation

CT cannot be considered superior to MRI or bone scintigraphy for diagnosing idiopathic osteonecrosis of the femoral head. However, there is weak evidence indicating that CT is superior for evaluating subchondral fractures, an important factor for staging. Its use is therefore weakly recommended.
Recommendation strength: 2, strength of evidence: D (very weak), agreement rate: 100% (10/10)

Background

Idiopathic osteonecrosis of the femoral head is recognized as a designated intractable disease by the Ministry of Health, Labour and Welfare. Because histological examination of biopsy samples is not 100% accurate, multiple approaches to diagnosis are needed, including diagnostic imaging. Staging and disease classification play major roles in clinical findings, treatment selection, and prognosis prediction; diagnosis incorporating them is also important.

In Japan, the diagnostic criteria and staging and disease classification of the working group of the Specific Disease Investigation Committee under the auspices of the Japanese Ministry of Health, Labour and Welfare's of idiopathic osteonecrosis of the femoral head have been authorized by the Japanese Orthopaedic Association and are widely used (secondary source 1). The diagnostic criteria incorporate conventional radiography, bone scintigraphy, MRI, and histology findings; staging classification uses conventional radiography findings; and disease classification uses conventional radiography and MRI findings (secondary source 1). Internationally, although there is a staging classification, there are no international diagnostic criteria, and the staging classification serves in this role. The frequently used

staging classification of the Association Research Circulation Osseous (ARCO) incorporates findings from conventional radiography, CT, bone scintigraphy, and MRI (secondary source 2).

The basis of the BQ statement and CQ recommendation grade for each imaging examination used to diagnose idiopathic osteonecrosis of the femoral head is explained below.

Explanation

There have been 8 articles reporting cross-sectional studies of the diagnostic performance of each type of imaging examination in idiopathic osteonecrosis of the femoral head and 1 meta-analysis of the diagnostic performance of MRI.[1-9)] A systematic review of these articles was conducted. The reference standards used in the studies were varied and included histological examination of biopsy specimens, intramedullary pressure, and 1 or several different imaging examinations. There were few studies of conventional radiography or CT. Consequently, a meta-analysis could not be performed. However, both sensitivity and specificity were found to be lower with conventional radiography than with the other imaging examinations. Conventional radiography sensitivity and specificity were 57% and 77%, respectively.[1)] CT sensitivity was 70.6% in 1 study[2)] and 92.7% in another.[3)] Bone scintigraphy sensitivity and specificity ranged from 60% to 91.3% and 79% to 100%, respectively.[1-6)] MRI (Fig.) sensitivity and specificity ranged from 50% to 100% and 71% to 100%, respectively.[1, 3-5, 7)]

Mitchell et al. compared the diagnostic performance of MRI, CT, and bone scintigraphy in an ROC analysis and reported that MRI provided the highest accuracy for early diagnosis.[8)] In a meta-analysis of the diagnostic performance of MRI in early idiopathic osteonecrosis of the femoral head by Zhang et al., sensitivity and specificity were both high, at 93.0% (95% CI, 92.0% to 94.0%) and 91.0% (95% CI, 89.0% to 93.0%), respectively, indicating that the diagnostic performance of MRI was high.[9)] In 2 studies that compared bone scintigraphy combined with SPECT and MRI, sensitivity was higher with bone scintigraphy (91% and 100%) than with MRI (87% and 66%).[4, 7)]

Figure　Idiopathic osteonecrosis of the femoral head

A: MRI, T1-weighted coronal image; B: MRI, T2-weighted sagittal image: Osteonecrosis is present in the anterosuperior area of the left femoral head, and band-like hypointensity suggestive of a necrotic border is seen (⟹). Linear hypointensity parallel to the articular surface is seen in the subchondral region of the anterosuperior area of the femoral head (▷), a finding indicative of subchondral fracture. This is accompanied by a hypointense region indicating bone marrow edema in the periphery of the necrosis (→).

C: CT, MPR, coronal image; D: CT, MPR, sagittal image: Subchondral fracture in the anterosuperior femoral head is identified as linear sclerotic changes (▷). Linear sclerotic changes are seen on the border with the osteonecrosis (⟹).

On the other hand, in a multicenter study of diagnostic performance in idiopathic osteonecrosis of the femoral head, Sugano et al. reported very high diagnostic performance (sensitivity of 91% and specificity of 99%) by combining any 2 of 5 criteria identified for conventional radiography, bone scintigraphy, MRI, and histology.[1)]

The above findings indicate that the diagnostic performance of bone scintigraphy combined with SPECT and MRI is high, and combining multiple tests is considered desirable. However, these studies have various problems that should be considered. These include the fact that they use a variety of reference standards, the MRI magnetic field strengths and imaging methods used vary, and many of the reports are old, and the performance of the imaging systems used differed from that of current systems.

With regard to staging, there were 5 articles reporting cross-sectional studies of the usefulness of imaging examinations,[10-14] and a systematic review of these articles was conducted. Lee et al. reported that the stage increased with the use of CT and MRI as compared with conventional radiography in 4 of 15 hip joints with idiopathic osteonecrosis of the femoral head.[10] In a comparison of staging according to the ARCO classification with the use of conventional radiography and MRI, Zibis et al. found that the sensitivity and specificity of conventional radiography using MRI as the reference standard were 88% and 90.5%, respectively, for stage II, 79.2% and 82%, respectively, for stage III, and 76% and 100%, respectively, for stage IV.[11] Moreover, the agreement rate between MRI and conventional radiography was 80.6% for staging, 71.2% for the location of the osteonecrotic lesion, 67.1% for the size of the osteonecrotic lesion, 79.2% for the presence of collapse of the articular surface, and 56.3% for degree of collapse.

Subchondral fracture in necrotic bone and collapse of the articular surface are important factors in staging. Sensitivity and specificity of 71% and 97%, respectively, were reported for conventional radiography in the evaluation of subchondral fracture, using CT as the reference standard.[12] Sensitivity of 38% and 92.9% and specificity of 100% and 28.6% were reported in 2 studies of MRI.[12, 13] Meier et al. compared the diagnostic performance of CT and MRI with respect to the presence and severity of subchondral fracture and collapse of the articular surface in ARCO classification stage III patients, using histology as the reference standard.[14] The detection rate for subchondral fracture was higher with CT (CT, 100%; MRI, 51%), and the extent of subchondral fracture and the severity of collapse could be evaluated more accurately with CT. CT was therefore reported to be superior to MRI for staging. Thus, although the evidence is weak, it indicates that CT is superior to conventional radiography and MRI for evaluating subchondral fractures in necrotic bone and the collapse of the articular surface. CT has also been used in preoperative planning in recent years.

Although the performance of conventional radiography in diagnosing idiopathic osteonecrosis of the femoral head is not very high, it is an imaging examination that results in little radiation exposure and permits inexpensive screening. High diagnostic performance is seen with MRI and bone scintigraphy combined with SPECT. Consequently, they are considered the standard imaging examinations. The diagnostic performance of CT cannot be considered superior to that of MRI or bone scintigraphy combined with SPECT, and CT results in radiation exposure. However, there is weak evidence that it is superior to those modalities for evaluating subchondral fracture in necrotic bone and collapse of the articular surface, which are important factors for staging. Its use is therefore weakly recommended.

Search keywords and secondary sources used as references

PubMed and the Cochrane Library database were searched for the period from 2016 to 2019 using the following keywords: femoral head, osteonecrosis, necrosis, radiography, bone scintigraphy, bone scan, CT, MRI, human, humans, sensitivity, specificity, and ROC. Although hits were obtained for 110 articles, only 1 article was extracted in secondary screening. Another 13 articles that provided evidence regarding the usefulness of imaging examinations in diagnosing idiopathic osteonecrosis of the femoral head were also included in the review. These were among the articles cited in the Diagnostic Imaging Guidelines 2016 for the CQ, "What types of diagnostic imaging are recommended for diagnosing femoral head osteonecrosis?"

In addition, the following were referenced as secondary sources.

1) The Japanese Orthopaedic Association; Ministry of Health, Labour and Welfare panel on the designated intractable disease idiopathic osteonecrosis of the femoral head; The Japanese Orthopaedic Association Panel on Clinical Practice Guidelines, Committee to Formulate Clinical Practice Guidelines for idiopathic osteonecrosis of the femoral head: 2019 Clinical Practice Guidelines for idiopathic osteonecrosis of the femoral head. Nankodo, 2019.
2) Yoon BH et al: The 2019 Revised Version of Association Research Circulation Osseous Staging System of Osteonecrosis of the Femoral Head. J Arthroplasty 35: 933-940, 2020
3) Japan Radiological Society, Ed.: Diagnostic Imaging Guidelines 2016. KANEHARA & Co., 2016.

References

1) Sugano N et al: Diagnostic criteria for non-traumatic osteonecrosis of the femoral head: a multicentre study. J Bone Joint Surg Br 81: 590-595, 1999
2) Coleman BG et al: Radiographically negative avascular necrosis: detection with MR imaging. Radiology 168: 525-528, 1988
3) Thickman D et al: Magnetic resonance imaging of avascular necrosis of the femoral head. Skeletal Radiol 15: 133-140, 1986
4) Stulberg BN et al: Multimodality approach to osteonecrosis of the femoral head. Clin Orthop Relat Res 240: 181-193, 1989
5) Markisz JA et al: Segmental patterns of avascular necrosis of the femoral heads: early detection with MR imaging. Radiology 162: 717-720, 1987
6) Lee EJ et al: Incidence and radio-uptake patterns of femoral head avascular osteonecrosis at 1 year after renal transplantation: a prospective study with planar bone scintigraphy. Nucl Med Commun 27: 919-924, 2006
7) Ryu JS et al: Bone SPECT is more sensitive than MRI in the detection of early osteonecrosis of the femoral head after renal transplantation. J Nucl Med 43: 1006-1011, 2002
8) Mitchell DG et al: Avascular necrosis of the hip: comparison of MR, CT, and scintigraphy. AJR Am J Roentgenol 147: 67-71, 1986
9) Zhang YZ et al: Accuracy of MRI diagnosis of early osteonecrosis of the femoral head: a meta-analysis and systematic review. J Orthop Surg Res 13: 167, 2018
10) Lee MJ et al: A comparison of modern imaging modalities in osteonecrosis of the femoral head. Clin Radiol 42: 427-432, 1990
11) Zibis AH et al: The role of MR imaging in staging femoral head osteonecrosis. Eur J Radiol 63: 3-9, 2007.
12) Stevens K et al: Subchondral fractures in osteonecrosis of the femoral head: comparison of radiography, CT, and MR imaging. AJR Am J Roentgenol 180: 363-368, 2003
13) Yeh LR et al: Diagnostic performance of MR imaging in the assessment of subchondral fractures in avascular necrosis of the femoral head. Skeletal Radiol 38: 559-564, 2009
14) Meier R et al: Bone marrow oedema on MR imaging indicates ARCO stage 3 disease in patients with AVN of the femoral head. Eur Radiol 24: 2271-2278, 2014

BQ 82 Is MRI recommended for diagnosing meniscal and cruciate ligament injuries of the knee joint?

Statement

MRI is useful and recommended for diagnosing meniscal and cruciate ligament injuries of the knee joint. However, it should not be performed alone, but rather in combination with an examination by an orthopedist that includes history-taking.

Background

There are many opportunities to use MRI to diagnose injuries of the menisci and cruciate ligaments, which are intra-articular structures. However, diagnosis based on manual testing by an orthopedist is also established, and some orthopedists think there is little need for MRI. Moreover, although the most reliable diagnostic method is arthroscopy, it is highly invasive and expensive compared with MRI. MRI should therefore be used for diagnosis instead of arthroscopy, if possible. The usefulness of MRI for diagnosing meniscal and cruciate ligament injuries is discussed below.

Explanation

Numerous cross-sectional studies have examined the performance of MRI in diagnosing meniscal and cruciate ligament injuries of the knee joint, using arthroscopy as the reference standard (Figs. 1 and 2). In a meta-analysis by Oei et al., MRI sensitivity and specificity were 93.3% (95% CI, 91.7% to 95.0%) and 88.4% (95% CI, 85.4% to 91.4%), respectively, for medial meniscal tears; 79.3% (95% CI, 74.3% to 84.2%) and 95.7% (95% CI, 94.6% to 96.8%), respectively, for lateral meniscal tears; 94.4% (95% CI, 92.3% to 96.6%) and 94.3% (95% CI, 92.7% to 95.9%), respectively, for anterior cruciate ligament tears; and 91.0% (95% CI, 83.2% to 98.7%) and 99.4% (95% CI, 98.9% to 99.9%), respectively, for posterior cruciate ligament tears.[1)] In a meta-analysis by Crawford et al., sensitivity, specificity, and the diagnostic accuracy rate were 91.4%, 81.1%, and 86.3%, respectively, for medial meniscal tears; 76.0%, 93.3%, and 88.8%, respectively, for lateral meniscal tears; and 86.5%, 95.2%, and 93.4%, respectively, for anterior cruciate ligament tears.[2)] In a meta-analysis by Phelan et al., MRI sensitivity and specificity were 89% (95% CI, 83% to 94%) and 88% (95% CI, 82% to 93%), respectively, for medial meniscal tears; 78% (95% CI, 66% to 87%) and 95% (95% CI, 91% to 97%), respectively, for lateral meniscal tears; and 87% (95% CI, 77% to 94%) and 93% (95% CI, 91% to 96%), respectively, for anterior cruciate ligament tears.[3)] Although MRI shows high diagnostic performance in meniscal and cruciate ligament injuries, its lowest sensitivity is for lateral meniscal tears. Consequently, when interpreting MRI, the lowest criterion for the presence of a tear in the lateral meniscus should be specified. The MRI systems used in the reports varied widely, from 0.1T to 1.5T. However, reports show that there are no differences in diagnostic performance depending on the magnetic field strengths of the systems.[4-6)]

Figure 1. Horizontal tear of the medial meniscus

MRI, $T2^*$-weighted sagittal image: A linear hyperintensity is seen extending to the inferior surface of the posterior horn of the medial meniscus (→).

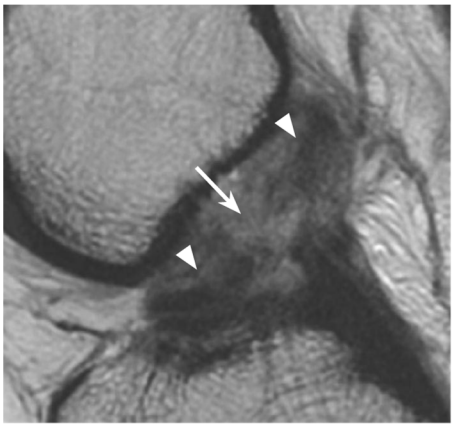

Figure 2. Complete tear of the anterior cruciate ligament

MRI, T2-weighted sagittal image: There is no continuity at the center of the anterior cruciate ligament (→), and swelling, hyperintensity, and deflection of the fragments are seen (▷).

Numerous cross-sectional studies have also examined the usefulness of manual testing in diagnosing meniscal and cruciate ligament injuries of the knee joint, using arthroscopy as the reference standard. Meta-analyses of these studies showed variability in the diagnostic performance of the various manual tests.[7, 8] However, in investigations regarding typical manual tests, a meta-analysis by Hegedus et al. of the McMurray test for meniscal injury showed sensitivity of 70.5% and specificity of 71.1%,[7] and a meta-analysis by Van Eck et al. of the Lachman test without anesthesia for diagnosing anterior cruciate ligament injury showed sensitivity and specificity of 81% each.[8] However, the shortcomings of arthroscopy include the fact that it is dependent on the skill of the operator; that some locations are difficult to observe, such as the margins and posterior segment of the meniscus; and that only the surface of intra-articular structures can be observed. It should therefore be kept in mind that arthroscopy is less than perfect as a reference standard.

Several cross-sectional studies have used arthroscopy as the reference standard in comparing the diagnostic performance of MRI with clinical findings obtained in examinations by orthopedists that included history-taking. However, the subjects in nearly all of these studies have been patients with suspected meniscal or ligament injuries based on clinical findings. Although there are reports indicating that the diagnostic performance of clinical findings is comparable to or higher than that of MRI,[9-13] there are also reports indicating that the diagnostic performance of MRI is higher than that of clinical findings,[14, 15] making it difficult to draw conclusions. However, after the orthopedist has examined the patient, the evaluation generally combines MRI with clinical findings rather than being based on MRI alone. Several cross-sectional studies examined whether diagnostic arthroscopy can be obviated by performing MRI in patients with suspected meniscal or ligament injuries based on clinical findings obtained in an examination

by an orthopedist. The results indicated that arthroscopy was reduced by 27.3% to 51.4% with the use of MRI.[16-18)]

MRI is useful for diagnosing meniscal and cruciate ligament injury and is recommended as a standard imaging examination for this purpose. However, it should preferably not be performed alone, but rather in combination with an examination by an orthopedist that includes history-taking.

Search keywords and secondary sources used as references

PubMed was searched for the period since 2012 using the following keywords: knee, meniscus injury, meniscus tear, ligament injury, ligament tear, MRI, and arthroscopy.

References

1) Oei EH et al: MR imaging of the menisci and cruciate ligaments: a systematic review. Radiology 226: 837-848, 2003
2) Crawford R, et al: Magnetic resonance imaging versus arthroscopy in the diagnosis of knee pathology, concentrating on meniscal lesions and ACL tears: a systematic review. Br Med Bull 84: 5-23, 2007
3) Phelan N et al: A systematic review and meta-analysis of the diagnostic accuracy of MRI for suspected ACL and meniscal tears of the knee. Knee Surg Sports Traumatol Arthrosc 24: 1525-1539, 2016
4) Vellet AD et al: Anterior cruciate ligament tear: prospective evaluation of diagnostic accuracy of middle- and high-fieldstrength MR imaging at 1.5T and 0.5T. Radiology 197: 826-830, 1995
5) Cotton A: MR imaging of the knee at 0.2T and 0.5T: correlation with surgery. AJR Am J Roentgenol 174: 1093-1097, 2000
6) Cheng Q, et al: Comparison of 1.5- and 3.0-T magnetic resonance imaging for evaluating lesions of the knee: a systematic review and meta-analysis (PRISMA-compliant article). Medicine 97: 38, 2018
7) Hegedus EJ et al: Physical examination tests for assessing a torn meniscus in the knee: a systematic review with meta-analysis. J Orthop Sports Phys Ther 37: 541-550, 2007
8) Van Eck CF et al: Methods to diagnose acute anterior cruciate ligament rupture: a meta-analysis of physical examinations with and without anaesthesia. Knee Surg Sports Traumatol Arthrosc 21: 1895-1903, 2013
9) Brooks S et al: Accuracy of clinical diagnosis in the knee arthroscopy. Ann R Coll Surg Engl 84: 265-268, 2002
10) Ryzewicz M et al: The diagnosis of meniscus tears: the role of MRI and clinical examination. Clin Orthop Relat Res 455: 123-133, 2007
11) Madhusudhan TR at al: Clinical examination, MRI and arthroscopy in meniscal and ligamentous knee Injuries: a prospective study. J Orthop Surg Res 3: 19, 2008
12) Rayan F et al: Clinical, MRI, and arthroscopic correlation in meniscal and anterior cruciate ligament injuries. Int Orthop 33: 129-132, 2009
13) Yan R et al: Predicted probability of meniscus tears: comparing history and physical examination with MRI. Swiss Med Wkly 141: w13314, 2011
14) Navali AM et al: Arthroscopic evaluation of the accuracy of clinical examination versus MRI in diagnosing meniscus tears and cruciate ligament ruptures. Arch Iran Med 16: 229-232, 2013
15) Munk B et al: Clinical magnetic resonance imaging and arthroscopic findings in knees: a comparative prospective study of meniscus anterior cruciate ligament and cartilage lesions. Arthroscopy 14: 171-175, 1998
16) Ruwe PA et al: Can MR imaging effectively replace diagnostic arthroscopy ? Radiology 183: 335-339, 1992
17) Bui-Mansfield LT et al: Potential cost saving of MR imaging obtained before arthroscopy of the knee. AJR Am J Roentgenol 168: 913-918, 1997
18) Vincken PW et al: Effectiveness of MR imaging in selection of patients for arthroscopy of the knee. Radiology 223: 739-746, 2002

BQ 83 Is MRI recommended for diagnosing bone tumors and tumor-like lesions?

Statement

The first imaging examination that should be performed is conventional radiography. MRI is useful for detecting lesions and evaluating pathological changes and local invasion. It is therefore recommended when a malignancy is suspected based on conventional radiography or when a treatment plan cannot be determined.

Background

Although conventional radiography is the first imaging examination performed to evaluate bone tumors and tumor-like lesions, the opportunities to use MRI are numerous. The usefulness of MRI for diagnosing bone tumors and tumor-like lesions and its indications were examined.

Explanation

Although various imaging examinations are used to diagnose bone tumors and tumor-like lesions, conventional radiography (Fig.) is the least expensive and most accessible test that can detect lesions and be used to analyze their histological characteristics, and it can be performed at any facility. Typical cases of benign lesions can often be diagnosed by conventional radiography alone; there is little need to add other imaging examinations in such cases, except when invasive treatment is considered.[1, 2)] However, evaluation of flat bones may be difficult with conventional radiography alone. Ma et al. compared the diagnostic performance of MRI (Fig.) alone and MRI combined with conventional radiography in distinguishing benign from malignant bone tumors and tumor-like lesions in 51 patients. They found that the sensitivity of both methods was very good for malignant lesions, with no difference in sensitivity between them.[3)] However, with MRI alone, there was a tendency to overestimate benign lesions as malignant lesions, whereas evaluation with the combination of conventional radiography and MRI improved specificity by 20% and diagnostic accuracy by 18%.

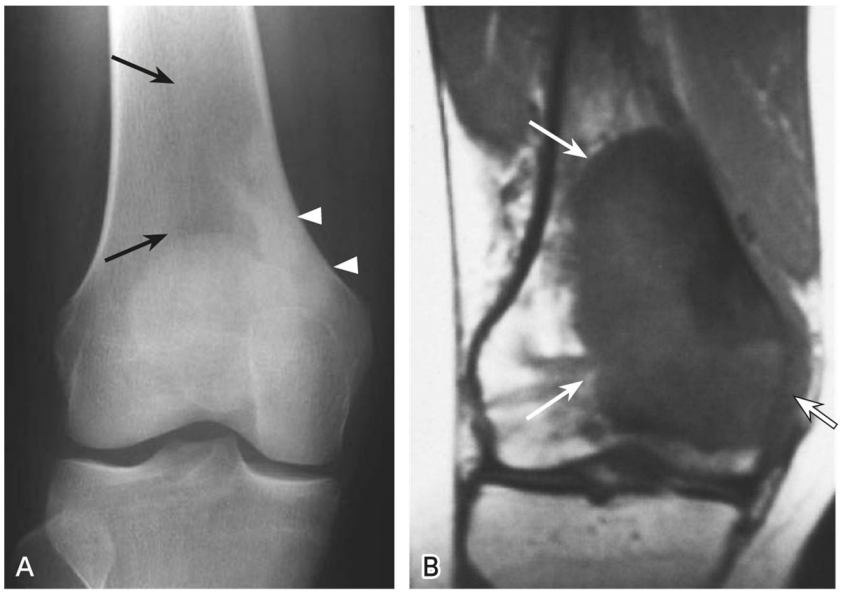

Figure Osteosarcoma

A: Plain radiograph, anteroposterior projection: An osteolytic lesion with indistinct borders is seen in the distal metaphysis of the right femur (→). Cloud-like calcification is seen inside the lesion (▷).

B: MRI, T1-weighted coronal image: An eccentric hypointense lesion is seen extending from the metaphysis to the epiphysis (⇨). The extent of the lesion's progression is clearer than in the plain radiograph.

Some studies have compared the performance of MRI and other diagnostic imaging modalities in determining the extent of bone tumors and tumor-like lesions. Hogeboom et al. compared CT and MRI in evaluating infiltration in 25 patients with bone tumors and tumor-like lesions. They reported that MRI was superior to CT in 25% of patients with bone marrow infiltration, 31% of patients with bone and soft tissue infiltration, and 36.4% of patients with joint infiltration.[4] In evaluating cortical bone destruction, however, CT was found to be useful and superior to MRI in 13.6% of the same group of patients. Zimmer et al. evaluated infiltration in 52 patients with bone tumors and tumor-like lesions and reported that MRI was superior to CT in 33% of patients with bone marrow infiltration and 38% of those with soft tissue invasion.[5] Bloem et al. compared MRI with CT and angiography in local staging of 56 patients with malignant bone tumors. They reported diagnostic sensitivity of 100% for MRI, 33% for CT, and 83% for angiography and specificity of 98% for MRI, 93% for CT, and 71% for angiography.[6] The investigators concluded that MRI was comparable to angiography for evaluating neurovascular infiltration and that MRI should be selected for the local staging of malignant bone tumors. Frank et al. compared the lesion detection performance of MRI and bone scintigraphy in 106 patients with clinically suspected malignant bone tumors and found the detection sensitivity of MRI to be significantly higher than that of bone scintigraphy.[7]

With regard to internal characterization, MRI, with its high contrast resolution, has been reported to be useful in a variety of diseases.[8-12] MRI can be used to infer the pathologies, such as fat, blood/hemosiderin, cartilage matrix, mucoid matrix, collagen fibers, and cysts, and it is useful for the qualitative diagnosis of

lesions. Mori et al. compared the diagnostic performance of MRI combined with conventional radiography and contrast-enhanced CT alone in 32 patients with bone tumors and tumor-like lesions. They reported that, although CT was superior for evaluating cortical bone destruction and calcification in lesions, the combination of MRI and conventional radiography was superior for analyzing the histological characteristics of lesions in 56% of the patients.[13)]

In the diagnosis of bone tumors and tumor-like lesions, MRI is useful for detecting lesions and evaluating pathological changes, and it is particularly good for evaluating local infiltration. However, CT is useful for evaluating cortical bone and calcification in lesions. For screening, conventional radiography is suitable, and MRI is recommended when a malignant tumor is suspected based on conventional radiography or when a treatment plan cannot be determined. When evaluating MRI, conventional radiography should be used as a reference.

Search keywords and secondary sources used as references

PubMed was searched using the following keywords: bone tumor and MRI.

In addition, the following were referenced as secondary sources.

1) Bestic JM et al: ACR Appropriateness Criteria®: primary bone tumors J Am Coll Radiol 17: S226-S238, 2020
2) Committee on Bone and Soft Tissue Tumors, Japanese Orthopaedic Association, Ed.: General Rules for Clinical and Pathological Studies on Malignant Bone Tumors, 4th Edition. KANEHARA & Co., 2015.

References

1) Sundaram M et al: Computed tomography or magnetic resonance for evaluating the solitary tumor or tumor-like lesion of bone? Skeletal Radiol 17: 393-401, 1988
2) Griffiths HJ et al: The use of MRI in the diagnosis of benign and malignant bone and soft tissue tumours. Australas Radiol 37: 35-39, 1993
3) Ma LD et al: Differentiation of benign and malignant musculoskeletal tumors: potential pitfalls with MR imaging. Radiographics 15: 349-366, 1995
4) Hogeboom WR et al: MRI or CT in the preoperative diagnosis of bone tumours. Eur J Surg Oncol 18: 67-72, 1992
5) Zimmer WD et al: Bone tumors: magnetic resonance imaging versus computed tomography. Radiology 155: 709-718, 1985
6) Bloem JL et al: Radiologic staging of primary bone sarcoma: MR imaging, scintigraphy, angiography, and CT correlated with pathologic examination. Radiology 169: 805-810, 1988
7) Frank JA et al: Detection of malignant bone tumors: MR imaging vs scintigraphy. AJR Am J Roentgenol 155: 1043-1048, 1990
8) Aoki J et al: MR findings indicative of hemosiderin in giant-cell tumor of bone: frequency, cause, and diagnostic significance. AJR Am J Roentgenol 166: 145-148, 1996
9) Cohen EK et al: Hyaline cartilage-origin bone and soft-tissue neoplasms: MR appearance and histologic correlation. Radiology 167: 477-481, 1988
10) Frick MA et al: Imaging findings in desmoplastic fibroma of bone: distinctive T2 characteristics. AJR Am J Roentgenol 184: 1762-1768, 2005
11) Murphey MD et al: Telangiectatic osteosarcoma: radiologicpathologic comparison. Radiology 229: 545-553, 2003
12) Campbell RS et al: Intraosseous lipoma: report of 35 new cases and a review of the literature. Skeletal Radiol 32: 209-222, 2003
13) Mori T et al: Three-dimensional images of contrast-enhanced MDCT for preoperative assessment of musculoskeletal masses: comparison with MRI and plain radiographs. Radiation Med 23: 398-406, 2005

CQ 22 Is contrast-enhanced MRI recommended for diagnosing soft tissue neoplasms and tumor-like lesions?

Recommendation

Although there is not a strong need for routine contrast-enhanced MRI, dynamic contrast-enhanced MRI is in some cases useful for distinguishing benign from malignant lesions, and contrast-enhanced MRI is therefore weakly recommended.

Recommendation strength: 2, strength of evidence: weak (C), agreement rate: 89% (8/9)

Background

MRI is a diagnostic imaging modality that plays the central role in diagnosing soft tissue neoplasms and tumor-like lesions. The Japan Radiological Society's Diagnostic Imaging Guidelines 2016 indicate that non-contrast MRI is useful for distinguishing benign from malignant lesions and for the qualitative diagnosis of benign masses, and they recommend that it be used in combination with clinical findings and conventional radiography. Contrast-enhanced MRI, on the other hand, has been said not to be useful for characterization because many solid tumors undergo enhancement over time. Consequently, opinions differ regarding the uniform use of contrast-enhanced MRI.[1, 2)]

This CQ discusses the usefulness of contrast-enhanced MRI for the qualitative diagnosis of soft tissue neoplasms and tumor-like lesions, the differentiation of benign and malignant lesions, and the histological diagnosis of the malignancy of soft tissue sarcomas.

Explanation

Contrast-enhanced MRI is used to differentiate between cysts and solid tumors for cyst-like soft tissue neoplasms and tumor-like lesions that show hyperintensity in T2-weighted images. Because diagnosing cysts is difficult, contrast-enhanced MRI is particularly useful when a lesion occurs at a site other than in the periphery of a joint, where cysts occur preferentially, and when a lesion shows non-uniform hyperintensity in T2-weighted images.[2, 3)] If a thick septum or nodule with contrast enhancement is seen in a lipoma, an atypical lipomatous tumor or well-differentiated liposarcoma is suspected.[4)] Dynamic contrast-enhanced MRI, which involves rapidly injecting contrast medium intravenously and repeatedly imaging in the same plane, is useful for internal characterization of components such as highly vascular components, which undergo enhancement early, and fibrous components, which undergo gradual enhancement, and thereby contributes to qualitative diagnosis.[5)]

With regard to the differentiation of benign and malignant lesions, van Rijswijk et al. conducted an investigation in 140 patients with soft tissue neoplasms or tumor-like lesions (benign in 67 patients, malignant in 73 patients) and reported sensitivity and specificity of 69% and 73%, respectively, with non-contrast MRI alone and 74% and 78%, respectively, with the addition of contrast-enhanced MRI.[6)]

With the further addition of dynamic contrast-enhanced MRI, sensitivity and specificity were 82% and 78%, respectively, the best results obtained. On the other hand, in an investigation in 39 patients with soft tissue neoplasms or tumor-like lesions (benign in 27 patients, malignant in 12 patients) by Grande et al., the addition of contrast-enhanced MRI to non-contrast MRI did not improve the diagnostic accuracy rate (decreased from 66% to 59%), but the addition of dynamic contrast-enhanced MRI improved it to 76%.[7] As the above findings indicate, there is still no established view regarding improvement in the ability to distinguish benign from malignant lesions with the addition of contrast-enhanced MRI to non-contrast MRI. However, sensitivity and specificity ranging from 64% to 96% and from 58% to 80%, respectively, were reported when tumors that underwent early-phase enhancement in dynamic contrast-enhanced MRI were considered malignant, indicating that dynamic contrast-enhanced MRI is to some extent useful for differentiating between benign and malignant lesions (Fig.).[5-9] Although variability was seen in the results, this was likely attributable to the sample sizes and the types of patients included in the studies. In addition, differences in the definition of early enhancement, the strength of the MRI magnetic field, and the MRI imaging parameters used should be considered. Because abnormal angiogenesis is often seen histopathologically in malignancies, the possibility of malignancy must be kept in mind for masses that undergo early enhancement in dynamic contrast-enhanced MRI. However, early enhancement in dynamic contrast-enhanced MRI is also seen in benign tumors and tumor-like lesions that undergo early enhancement, such as hemangiomas, glomus tumors, and acute myositis ossificans. It is therefore important to first exclude early-enhancing benign lesions by conventional radiography or non-contrast MRI, in addition to clinical information, and then focus on early enhancement in dynamic contrast-enhanced MRI.

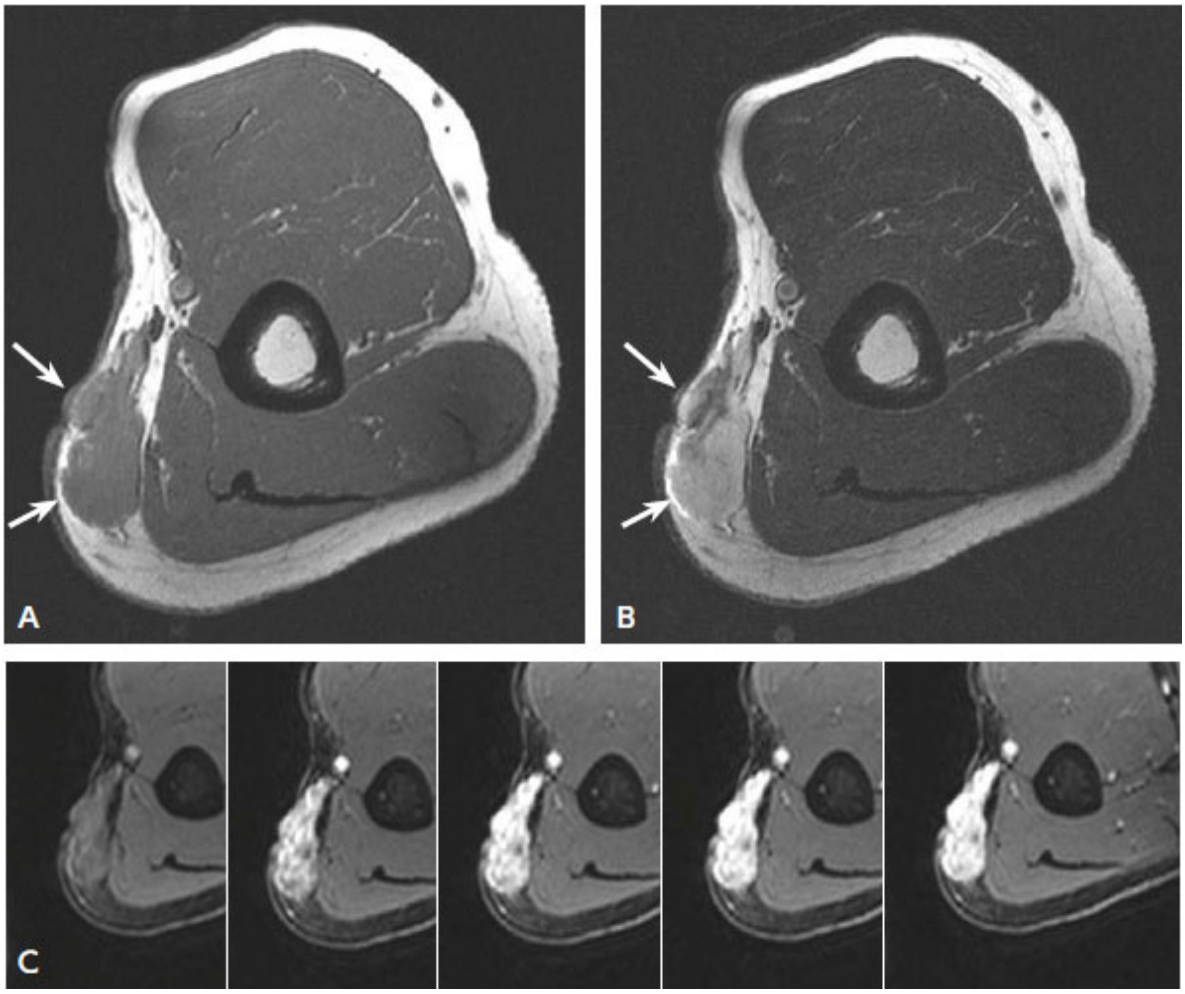

Figure Myxofibrosarcoma

A: MRI, T1-weighted image; B: MRI, T2-weighted image; C: Dynamic contrast-enhanced MRI
A subcutaneous mass with irregular margins is seen in the left brachial region (→). It is seen as isointensity compared with muscle on the T1-weighted image and as hyperintensity on the T2-weighted image. In dynamic contrast-enhanced MRI, the mass shows rapid initial enhancement, followed by sustained late enhancement.

With regard to the histological diagnosis of the malignancy of soft tissue sarcomas, Zhao et al. examined the MRI findings of 95 patients with soft tissue sarcomas and found that, when tumors that showed peritumoral enhancement were considered, the high-grade group (grades 2 and 3), sensitivity and specificity were 91% and 57%, respectively.[10] A multivariate analysis of 130 patients with soft tissue sarcoma by Crombé et al. showed that peritumoral enhancement, intratumoral necrosis, and heterogeneity of ≥ 50% in T2-weighted images were findings suggestive of high malignancy (grade 3). They reported that combining any 2 of these findings resulted in sensitivity and specificity of 75% and 64.2%, respectively.[11] In investigations in which the signals from tissues were imaged at high temporal resolution after contrast medium administration, and perfusion MRI was used to quantitatively analyze perfusion (hemodynamics at the capillary level), the transfer rate constant for leakage of the contrast medium into the extracellular space

(K^{trans}) was significantly higher in the high-grade group (grades 2 and 3) than in the low-grade group (grade 1).[12, 13)]

These findings indicate that contrast-enhanced MRI is useful for differentiating between cystic and solid tumors. Early enhancement in dynamic contrast-enhanced MRI is in some cases useful for differentiating benign from malignant tumors. Peritumoral enhancement may be useful in the histological diagnosis of the malignancy of soft tissue sarcomas. Contrast-enhanced MRI is weakly recommended for diagnosing soft tissue neoplasms and tumor-like lesions.

Search keywords and secondary sources used as references

PubMed and the Cochrane Library database were searched for the period from 2016 to 2019 using the following keywords, and selections were made from among 212 articles: soft tissue tumor, soft tissue tumor-like lesion, conventional MRI, contrast-enhanced MRI, dynamic contrast-enhanced MRI, sensitivity, and specificity. In the secondary screening, 10 articles were extracted, and 6 articles were added with a hand search.

In addition, the following was referenced as a secondary source.

1) Japan Radiological Society, Ed.: Diagnostic Imaging Guidelines 2016. KANEHARA & Co., 2016.

References

1) May DA et al: MR imaging of musculoskeletal tumors and tumor mimickers with intravenous gadolinium: experience with 242 patients. Skeletal Radiol 26: 2-15, 1997
2) Kransdorf MJ et al: The use of gadolinium in the MR evaluation of soft tissue tumors. Semin Ultrasound CT MR 18: 251-268, 1997
3) Ma LD et al: Differentiation of benign from malignant musculoskeletal lesions using MR imaging: pitfalls in MR evaluation of lesions with a cystic appearance. AJR Am J Roentgenol 170: 1251-1258, 1998
4) Panzarella MJ et al: Predictive value of gadolinium enhancement in differentiating ALT/WD liposarcomas from benign fatty tumors. Skeletal Radiol 34: 272-278, 2005
5) van der Woude HJ et al: Musculoskeletal tumors: does fast dynamic contrast-enhanced subtraction MR imaging contribute to the characterization? Radiology 208: 821-828, 1998
6) van Rijswijk CS et al: Soft-tissue tumors: value of static and dynamic gadopentetate dimeglumine-enhanced MR imaging in prediction of malignancy. Radiology 233: 493-502, 2004
7) Del Grande F et al: Characterization of indeterminate soft tissue masses referred for biopsy: What is the added value of contrast imaging at 3.0 tesla? J Magn Reson Imaging 45: 390-400, 2017
8) Tuncbilek N et al: Dynamic contrast enhanced MRI in the differential diagnosis of soft tissue tumors. Eur J Radiol 53: 500-505, 2005
9) Barile A et al: Musculoskeletal tumours: preliminary experience with perfusion MRI. Radiol Med 112: 550-561, 2007
10) Zhao F et al: Can MR imaging be used to predict tumor grade in soft-tissue sarcoma? Radiology 272: 192-201, 2014
11) Crombé A et al: Soft-tissue sarcomas: assessment of MRI features correlating with histologic grade and patient outcome. Radiology 291: 710-721, 2019
12) Li X et al: Soft tissue sarcoma: can dynamic contrast-enhanced (DCE) MRI be used to predict the histological grade? Skeletal Radiol 49: 1829-1838, 2020
13) Gondim Teixeira PA et al: Perfusion MR imaging at 3-tesla: can it predict tumor grade and histologic necrosis rate of musculoskeletal sarcoma? Diagn Interv Imaging 99: 473-481, 2018